Optimal Design and Operation of an Industrial Three Phase Reactor for the Oxidation of Phenol

Awad E. Mohammed, Aysar T. Jarullah[1,2] , Saba A. Gheni[1], Iqbal M. Mujtaba[3]

[1] Chemical Engineering Department, College of Engineering, Tikrit University

[2] Email: A.T.Jarullah@tu.edu.iq

[3] Chemical & Process Engineering Division, School of Engineering, University of Bradford, Bradford BD7 1DP UK

[3] Email: I.M.Mujtaba@bradford.ac.uk

Abstract

Among several treatment methods Catalytic Wet Air Oxidation (CWAO) treatment is considered as a useful and powerful method for removing phenol from waste waters. In this work, mathematical model of a trickle bed reactor (TBR) undergoing CWAO of phenol is developed and the best kinetic parameters of the relevant reaction are estimated based on experimental data (from the literature) using parameter estimation technique. The validated model is then utilized for further simulation and optimization of the process. Finally, the TBR is scaled up to predict the behavior of CWAO of phenol in industrial reactors. The optimal operating conditions based on maximum conversion and minimum cost in addition to the optimal distribution of the catalyst bed is considered in scaling up and the optimal ratio of the reactor length to reactor diameter is calculated with taking into account the hydrodynamic factors (radial and axial concentration and temperature distribution).

Key words: Catalytic Wet Air Oxidation; Phenol; Trickle bed reactor; Parameter estimation technique; Scaled-up

1. Introduction

Wastewater is composed of organic, inorganic compounds and dissolved gases. A major problem over the last decades is the groundwater contamination via organic chemical compounds resulting in huge public concern. These compounds constitute a very large group of pollutants present in the wastewater. Among these groups, the aromatic compounds especially phenol and its derivatives are the most common pollutants found in many industrial effluents (**Singh et al., 2004**). Phenols belong to the class of aromatic compounds having a hydroxyl group as well as any additional organic groups on a six-carbon benzene ring (**Qinglin and Karl, 1998**). Also, phenols are extremely toxic to aquatic life and resistance to biodegradation and have a strong unpleasant odor and taste in water even at concentrations in the parts per billion range (**Massa et al., 2004**).Generally, aqueous wastes have an organic pollutant load in the range of 500-10000 ppm and are too dilute to incinerate but yet too toxic. The major problems caused by phenol can be listed below (**Budavari, 1996; Lin, et al., 2006; Vázquez et al., 2007**):

- Phenols are persistent pollutants involving great damage to environment. They have been designated as priority pollutants.
- Phenols are very dangerous, harmful and toxic displaying toxic effects on aquatic life as well as its effect depend on the concentration of pollutants.

- Phenols may cause harmful effects on the central nervous system and heart, resulting in dysrhythmia, seizures and coma.
- The kidneys may be affected as well. Long-term or repeated exposure of the substance may have harmful effects on the liver and kidneys.
- Phenol and its vapors are corrosive to the eyes, the skin, and the respiratory tract. Its corrosive effect on skin and mucous membranes is due to a protein-degenerating effect.
- Repeating or prolonging skin contact with phenol may cause dermatitis, or even second and third degree burns. Chemical burns from skin exposures can be decontaminated by washing with polyethylene glycol, isopropyl alcohol, or perhaps even copious amounts of water.
- Systemic poisoning can occur in addition to the local caustic burns due to the quickly absorbed phenol through the skin.
- The phenols effluent to rivers and oceans reducing the light penetration and this effect on the organisms and plants found inside these waters.
- Phenol can give disagreeable tastes and odors to drinking water even at very low concentration. Phenol gives off a sweet, acrid smell detectable to most people at 40 ppb in air and at about 1–8 ppm in water.
- Phenol is also a reproductive toxin causing increased risk of abortion and low birth weight indicating retarded development in utero.

The concentration of phenol as organic pollutant presents in wastewater in various industries are: refineries (6-500 mg/l), cooking process (27-3900 mg/l), coal processing (9-6800 mg/l), petrochemicals (28-1220 mg/l), pharmaceutical, wood products, paint and pulp and paper industries (0.1-1600 mg/l) (**Busca et al., 2008**).Phenol is produced at a rate of about 6 million ton/year worldwide, with a significant increasing trend in the near future (**Jordan et al., 1991**). The Indian Ministry of Environment and Forests (MOEF) and Environmental Protection Agency (EPA) have listed phenol and phenolic compounds on the priority pollutants list. Despite the legislative restrictions, large amount of phenolic compounds are still being discharged into the environment. For example, in Europe 900 ton/year of phenols are directly or indirectly discharge to the water body (**Busca et al., 2008**). Due to high toxicity and difficult biodegradability, the MOEF has set a maximum concentration level of 1.0 mg/l of phenol in the industrial effluents for safe discharge into surface water.

To detoxify these organic contaminants from groundwater or to separate of pollutants present in polluted water became a major focus of research and policy debate. The presence of these pollutants in the water even at low concentrations does not allow reuse of the water in the industrial operations (**Mangrulkar et al., 2008**).Conventional process of removing these pollutants and especially phenols from wastewater is known as catalytic wet air oxidation (CWAO).Kinetics of CWAO of phenol have been studied by several researchers and tested experimentally for developing such process.

Pintar and Levec (**1992)** worked on CWAO of phenol in a trickle bed reactor using CUO, Zn, CO oxides as a heterogeneous catalyst and pure oxygen as oxidant. **Fortuny et al. (1998)** studied CWAO of phenol in a fixed bed reactor operating in a trickle flow regime using active carbon and commercial copper oxide supported over γ-alumina as a catalyst. **Eftaxias et al. (2001)** have investigated the CWAO of phenol upon a $CuO/\gamma - AL_2O_3$ as a catalyst in a continuous trickle bed reactor using air as oxidant. **Oscar et al. (2007)** studied experimentally the degradation of phenol in polluted water via UV/H_2O_2.**Wadood and Sama (2008)** have studied the CWAO of phenol oxidized in a fixed bed reactor working in trickle flow regime employing copper based catalyst supported on ɣ-alumina as a catalyst, and air as oxidant. **Keav et al. (2010)** investigated the CWAO of phenol tested in a fixed bed reactor over platinum and ruthenium catalysts supported on cerium-based oxides. **Wadood (2014)** studied the oxidation of phenol

in a trickle bed reactor using activated carbon as a catalyst under different conditions(pH, gas flow rate, LHSV, temperature and oxygen partial pressure).

Based on experimental studies with a homemade catalyst, the aim of this study is to develop kinetic models based on experimental data taken from literature for the CWAO process. For this purpose a full process model from the literature is used and the kinetic parameters of the model are estimated via minimizing sum of the squared error between the experimental data and the model predictions to find the best kinetic parameters. Pure oxygen (O_2) is used as an oxidant and ($\mathrm{Pt}/\gamma - Al_2O_3$) is used as a catalyst under the following operating conditions (temperature (120, 140, and 160℃), oxygen partial pressure (0.8, 1 and 1.2 MPa), liquid hourly space velocity (1, 2 and $3hr^{-1}$), initial phenol concentration (1, 3 and $5gm/l$) and gas flow rate (stoichiometric excess) (20, 40, 80 and 100%).Two approaches (linear and non-linear methods)have been used in evaluating the optimal kinetic parameters. The validated process model is then employed to scale up and to find the optimal design of an industrial reactor. The modeling, simulation and optimization process of CWAO operation are carried out using gPROMS software.

2. The Experimental Data

The experimental data have been taken from **Safaa (2009**). A brief description about the materials, apparatus and experimental procedure used for getting the experimental results can be summarized as follows:

Phenol in wastewater is oxidized in a trickle bed reactor as a main apparatus in the unit process, which is characterized in Table 1. Pure oxygen is used as an oxidant introduced as co-currently with phenol into the reactor packed with a fixed bed of catalyst (0.48 wt% $\mathrm{Pt}/\gamma - Al_2O_3$) characterized in Table 2.

CWAO of phenol and oxygen occurs with a solid catalyst and this reaction can happen along the catalyst bed that enclosed between two layers of inert material at the reaction conditions. The exit solution from the reactor goes to the gas-liquid separation for sampling. The experimental concentrations of phenol have been measured using JASCO ultraviolet/visible (UV-VIS/530) spectrophotometer (**Safaa 2009**). The schematic representation of the experimental equipment is represented in Figure 1. Calibration has been conducted on all laboratory equipment (such as pump, instrumentation and control) to ensure the accuracy of the measurements. Note, all analytical techniques that have been employed for the properties of the feedstock and the products were accurate, fast and repeatable. Product analysis was repeated twice for each sample at each operating condition to ensure the accuracy of the results. Average results have been taken into accounts for each run with maximum deviation of 2% among all runs.

3. Mathematical Model of Trickle Bed Reactor

Mathematical model is a set of ordinary algebraic and differential equations related to mass and energy balance and thermphysical properties of a system. The basic mathematical model for a chemical reaction rate should take into account the rate of mass and heat transfer together with the kinetic equation (**Jarullah, 2011; Nawaf, 2015**). In this work, the mathematical model of CWAO of phenol in a trickle bed reactor assumes plug flow and is based on two film theory (**Al-Dahhan et al., 1997**). The model for a trickle-bed catalytic reactor can be complex due to many microscopic and macroscopic effects occurring inside the reactor, including flow patterns of both phases, size and shape of a catalyst particles, wetting of the catalyst pores with liquid phase, pressure drop, intra-particle gradients, thermal effects and of course kinetics on the catalyst surface **(Jarullah et al., 2011a, 2011b, 2011c)**. Figure 2 shows the required data and available tools for modelling and simulation of CWAO of phenol process.

Mass Balance in Gas Phase

Equation (1) relates the concentration of oxygen and the mass transfer across the gas–liquid interface which gives the concentration profile of oxygen along the catalyst bed length (**Qiang et al., 2009**).

Oxygen:

$$\frac{dC_{O2,G}}{dz} = -\left(\frac{k_{GL}a_{GL}}{u_g}\right)\left(\frac{C_{O2,G}}{H_{O2}} - c_{O2,L}\right) \quad \textbf{(1)}$$

Mass Balance in Liquid Phase

The mass balance equations for the concentrations of phenol and oxygen in the liquid phase can be described by the following equations (**Qiang et al., 2009**):

Phenol:

$$\frac{dC_{ph,L}}{dz} = -\left(\frac{\eta_{LS}k_{LS}a_{LS}}{u_l}\right)\left(C_{ph,L} - C_{ph,L-s}\right) \quad \textbf{(2)}$$

Oxygen:

$$\frac{dC_{O2,G}}{dl} = \left(\frac{k_{GL}a_{GL}}{u_l}\right)\left(\frac{C_{O2,G}}{H_{O2}} - C_{O2,L}\right) - \left(\frac{\eta_{LS}k_{LS}a_{LS}}{u_l}\right)\left(C_{O2,L} - C_{O2,L-s}\right) \quad \textbf{(3)}$$

Mass Balance in Solid Phase

To solve the obove equations, the concentrations of phenol and oxygen at the solid surface are required, which are described by the two followingequations relating the extent of chemical reactions at the solid surface. At steady–state, the compounds transported between the liquid and solid phase (on the surface of the catalyst) are consumed or produced through the chemical reaction.

Phenol:

$$k_{LS}a_{LS}\left(C_{ph,L} - C_{ph,L-S}\right) = \eta_0\,(1-\varepsilon_B)R_{ph} \quad \textbf{(4)}$$

Oxygen:

$$k_{LS}a_{LS}\left(C_{O2,L} - C_{O2,L-S}\right) = 7\eta_0(1-\varepsilon_B)R_{ph} \quad \textbf{(5)}$$

The required boundary conditions are as follow:

$C_{ph,L}$ (at Z =0) = $C_{ph,L}$ (initial) **(6)**

$C_{O2,G}$ (at Z =0) = $C_{O2,G}$ (initial) **(7)**

$C_{O2,L}$ (at Z =0) = 0 **(8)**

Chemical Reaction Rate

The catalytic wet air oxidation can be described by the following kinetic equation of Langmuir–Hinshelwood type that accounts for phenol disappearance as shown below (**Qiang et al., 2009**):

$$R_{ph} = \rho_{cat}K_{het}\frac{{C_{ph}}^n{C_{O2}}^m}{\left(1+K_{ph}C_{ph,L}\right)^2} \quad \textbf{(9)}$$

The adsorption equilibrium constant of phenol (K_{ph}) is evaluated by the following relation (**Qiang et al., 2009**):

$$K_{ph} = \exp\left(-\frac{364.47}{T} - 2.3854\right) \quad \textbf{(10)}$$

Reaction rate constant (K_{het}) can be described by Arrhenius equation as follows :

$$K_{het} = A^0 \exp\left(-\frac{EA}{RT}\right) \quad \textbf{(11)}$$

Gas–Liquid Mass Transfer Coefficients

Gas-Liquid mass transfer coefficients can be evaluated by (**Rodriguez and Ancheyta, 2004; Mederos et al., 2006**) as follows:

Phenol:

$$\frac{K_{O2}^{L} a_L}{D_{O2}^{L}} = 7\left(\frac{\rho_{ph}\, u_l}{\mu_{ph}}\right)^{0.4} \left(\frac{\mu_{ph}}{\rho_{ph}\ D_{O2}^{L}}\right)^{0.5} \quad \textbf{(12)}$$

Liquid–Solid Mass Transfer Coefficients

Liquid- solid mass transfer coefficient can be evaluated from Van Krevelen–Krekels equations (**Froment and Bischoff, 1990; Bhaskar and Valavarasu, 2002**):

Phenol:

$$\frac{K_{ph}^{S}}{D_{ph}^{L} a_{LS}} = 1.8\left(\frac{\rho_{ph} u_l}{a_{LS}\mu_{ph}}\right)^{0.5} \left(\frac{\mu_{ph}}{\rho_{ph} D_{ph}^{L}}\right)^{(1/3)} \quad \textbf{(13)}$$

Oxygen:

$$\frac{K_{O2}^{S}}{D_{O2}^{L}\, a_{Ls}} = 1.8\left(\frac{\rho_{ph} u_l}{a_{Ls}\mu_{ph}}\right)^{0.5} \left(\frac{\mu_{ph}}{\rho_{ph} D_{O2}^{L}}\right)^{(1/3)} \quad \textbf{(14)}$$

Molecular Diffusivity

The molecular diffusivity of phenol and oxygen can be calculated by **Tyn-callus's** correlation (**Reid et al., 1987; Dudukovic et al., 2002**):

Phenol:

$$D_{ph}^{L} = 8.93 \times 10^{-8} \frac{v_L^{0.267}\ T}{v_{ph}^{0.267} \mu_{ph}} \quad \textbf{(15)}$$

Oxygen:

$$D_{O2}^{L} = 8.93 \times 10^{-8} \frac{v_L^{0.267}\ T}{v_{O2}^{0.267} \mu_{ph}} \quad \textbf{(16)}$$

The molar volume of liquid (v_L), phenol (v_{ph}) and oxygen (v_{O2}) can be calculated using the following equations (**Dudukovic et al., 2002; Jarullah et al., 2011a, 2011b**):

Liquid: $v_L = 0.285\ (v_c^{\,L})^{1.048}$ **(17)**

Phenol: $v_{ph} = 0.285\ (v_c^{\,ph})^{1.048}$ **(18)**

Oxygen: $v_{O2} = 0.285\ (v_c{}^{O2})^{1.048}$ **(19)**

The value of critical volume of liquid ($v_c{}^{L}$), phenol ($v_c{}^{ph}$) and oxygen ($v_c{}^{O2}$) can be found from **Perry and Green, (1999)**, which are listed in Table (4).

Henry's constant

Henry's constant for oxygen component (O_2) is calculated from the following equation (**Qianget al., 2009**):

$$H_{O2} = (6088.8 - 871.2\ ln\ T - \frac{326284}{T}) \quad \textbf{(20)}$$

Density of Phenol

The density of phenol can be evaluated by using (**Rackett, 1970)**:

$$\rho_{ph} = \frac{MW_{ph} P_c}{R\ T_C Z_C (1+(1-T_r)^{2/7}} \quad \textbf{(21)}$$

$$T_r = \frac{T}{T_c} \quad \textbf{(22)}$$

T_c , P_c and Z_c are estimated from **Perry and Green (1999)**.

Density of oxygen

The density of oxygen (O_2) can be estimated depending on the temperature and pressure from the ideal gas equation taking into considerations the gas compressibility factor, where the gas at these condition having a trend toward the reality state. The equation can be written as:

$$\rho_{O2} = \frac{P\ MW_{O2}}{Z_{O2}\ R\ T} \quad \textbf{(23)}$$

Viscosity of Phenol

The viscosity of phenol depends mainly on temperature (inversely proportion), thus, it is particularly desirable to determine liquid viscosities from experimental data when such data exist. Many correlations were used to calculate liquid viscosity and one of the best correlations that have widely been applied in calculating liquid viscosity (**Bruce et al., 2004**) is:

$$\mu_{ph} = \exp\left(ln(\propto \times \mu_{ph,b}) \times \left(\frac{ln(\mu_{ph,b})}{ln(\propto \times \mu_{ph,b})} \right)^{\emptyset} \right) \quad \textbf{(24)}$$

$$\emptyset = \frac{1-T_r}{1-T_{br}} \quad \textbf{(25)}$$

$$T_r = \frac{T}{T_C} \quad \textbf{(26)}$$

$$T_{br} = \frac{T_b}{T_C} \quad \textbf{(27)}$$

Effectiveness Factor

The effectiveness factor can be estimated as a function of Thiel Modulus, which is valid for sphere particle (**Marroquin et al., 2005**).

$$\eta_0 = \frac{3(\varphi coth\varphi - 1)}{\varphi^2} \quad \textbf{(28)}$$

For n^{th}- order irreversible reaction, the general Thiel Modulus (φ) is evaluated using the following relationship (**Froment and Bischoff, 1990; Nawaf et al., 2015a, 2015c**):

$$\varphi = \frac{V_P}{S_P}\sqrt{\left(\frac{n+1}{2}\right)\left(\frac{K_{het}C_{ph}^{n-1}\rho_p}{D_{ei}}\right)} \quad \textbf{(29)}$$

The Particle density (ρ_p), is determined using the following simple relation:

$$\rho_p = \frac{\rho_{cat.}}{1-\epsilon_B} \quad \textbf{(30)}$$

The Bed porosity (ϵ_B) of the catalyst is estimated for undiluted sphere packed catalyst from the following equation (**Haughey and Beveridge, 1969; Froment and Bischoff, 1990**).

$$\epsilon_B = 0.38+0.073\left(1 + \frac{(\frac{d_t}{d_{pe}} - 2)^2}{(\frac{d_t}{d_{pe}})^2}\right) \quad \textbf{(31)}$$

Equivalent particle diameter (d_{pe}), can be defined as the diameter of the sphere that has the same external surface (or volume) as the actual catalyst particle. This characteristic of the particle is very important and depends on the particle size and shape.

$$d_{pe} = d_p = 1.6 \text{ mm} \quad \textbf{(32)}$$

For spherical shape of particle, the external volume (V_p) and the surface area (S_P) of particle can be calculated as shown below:

$$V_p = \frac{4}{3}\pi(r_P)^3 \quad \textbf{(33)}$$

$$S_P = 4\pi(r_P)^2 \quad \textbf{(34)}$$

The surface area of particle per unit volume of the bed is evaluated as (**Froment and Bischoff, 1990**):

$$a_{LS} = \frac{S_P(1-\epsilon_B)}{V_p} \quad \textbf{(35)}$$

The effective diffusivity (D_{ei}), can be calculated from (**Jarullah et al., 2011c; Nawaf et al., 2015c**) taking into account the consideration of porosity and tortuosity of the pore network inside the particle.

$$D_{ei} = \frac{\epsilon_S}{\text{Ծ}}\frac{1}{\frac{1}{D_{mo,i}} + \frac{1}{D_{kn,i}}} \quad \textbf{(36)}$$

Catalyst particle porosity (ϵ_S) is estimated using equation below depending on the particle density and pore volume.

$$\epsilon_S = \rho_p V_g \quad \textbf{(37)}$$

The tortuosity factor (Ծ), has a values of 2 to 7 (**Satterfield, 1975**). According to literatures, the tortuosity factor is assumed to be 4 (**Satterfield, 1975; Marroquin et al., 2005**).

Knudsen diffusivity ($D_{kn,i}$, $cm^2/sec.$) can be calculated from the following equation (**Jarullah et al., 2012a; Froment and Bischoff, 1990**) as follows:

$$D_{kn,i} = 9700\, r_g \sqrt{\frac{T}{MW_{ph}}} \quad \textbf{(38)}$$

Mean pore radius (r_g), can be estimated as follows (**Nawaf et al., 2015a, 2015b):**

$$r_g = 2\frac{V_g}{S_g} \quad \textbf{(39)}$$

4. Estimation of Kinetic Parameters of the Model

The solution of transport problems in three-phase systems is very complex and usually numerical approximation methods are used. On the other hand, analytical solutions are used for the simple models. Thus, the boundary conditions proposed for these models need a careful attention (**Feike and Toride, 1998**).

Many physiochemical processes are described by systems of equations with unknown parameters which need to be estimated accurately. However, parameter estimation is a difficult step in the development of process models and requires experimental data. It is based on minimum errors between the measured experimental data and the predicted data from the mathematical model (**Poyton et al., 2006; Jarullah et al., 2011e; Sameer et al., 2016**). In order to evaluate the best values of kinetic parameters in this study, two approaches have been employed depending on phenol content in the oxidation process under varied operating conditions. These are as follows:

- Linear regression to simultaneously obtain the reaction orders of phenol (n), oxygen (m) and reaction rate constants (K_{het}), then linear regression with the Arrhenius equation to estimate the activation energy (EA) and pre-exponential factor (A^0).
- Non-linear regression to determine reaction orders of phenol (n), and oxygen (m) and after that estimation of activation energy (EA) and pre-exponential factor (A^0) .

Both approaches are based upon the minimization of the sum of squared errors (SSE) between the experimental and predicted concentrations of phenol ($C_{ph}^{exp.}, C_{ph}^{pred.}$) defined as:

$$\text{SSE} = \sum_{n=1}^{N_t} (C_{ph}^{exp.} - C_{ph}^{pred.})^2 \quad \textbf{(40)}$$

Following optimization problems are developed to estimate the kinetic parameters:

4.1 Optimization Problem Formulation for Parameter Estimation:

The optimization problem formulation for the catalytic oxidation process of phenol can be stated as follows:

Given	The reactor configuration, the initial phenol concentration, the catalyst, reaction temperature, oxygen partial pressure, liquid hourly space velocity and gas flow rate.
Obtain	The reaction orders of phenol (n), oxygen (m) and also reaction rate constants (K_{het}) at each temperature.
So as to minimize	The sum of square errors (SSE).
Subjected to	Process constraints and linear bounds on all optimization variables in the process.

Mathematically, employing the first approach the problem can be represented as follow:

Min SSE

$n, m, K_{het,i}$

s.t. f(z, x(z), $\tilde{x}$(t) , u(z), v) = 0 , [z_0, z_f] [Model, equality constraint]

$$n^L \leq n \leq n^U$$ [Inequality constraint]

$$m^L \leq m \leq m^U$$ [Inequality constraint]

$$K_{het,i}^L \leq K_{het,i} \leq K_{het,i}^U$$ [Inequality constraint]

While, using the second approach, the problem can be described as shown below:

Min SSE

n, m, E_A, A^0

s.t. f(z, x(z), $\tilde{x}$(z) , u(z), v) = 0 , [z_0, z_f] [model, equality constraint]

$$n^L \leq n \leq n^U$$ [Inequality constraints]

$$m^L \leq m \leq m^U$$ [Inequality constraint]

$$EA^L \leq EA \leq EA^U$$ [Inequality constraint]

$$A^{0L} \leq A^0 \leq A^{0U}$$ [Inequality constraint]

Where, f(z, x(z), $\tilde{x}$(z), u(z), v) = 0 Represents the process model presented in section 3, *.z* is the length of the reactor bed (independent variable). u(z) is the decision variables (*n*, *m*, EA, A^0), x(z) Gives the set of all differential and algebraic variables ($C_{O2,G}$, $C_{ph,L}$, $R_{ph,V}$, ….),$\tilde{x}$(z) Represents the derivative of differential variables with respect to length of the bed of reactor such as ($\frac{dC_{O2,G}}{dl}$, $\frac{dC_{ph,L}}{dl}$, …..).*V* is the constants parameters or design variables such as (*R*, …).[z_0, z_f], is the length interval of interest.The function *f* is assumed to be continuously differentiable with respect to all its arguments (**Jarullah et al., 2013; Jarullah et al., 2015**).

The method used for the solution of the above optimization problems by gPROMS is based on two steps as follows:

- The first step performs a simulation to converge all the equality constraints (function f) and also to calculate the inequality constraints.
- The second step performs the optimization (updates the values of the decision variables such as the kinetic parameters).

The above two steps are executed in repetitive manner until the SSE is minimized satisfying all the constraints.

5. Scale Up to an Industrial Trickle Bed Reactor

Trickle bed reactors (TBRs) have been widely used in numerous industrial applications for more than 70 years. They are applied in different chemical processes such as catalytic conversion. Although new structured catalysts and reactors have been developed, the packed bed reactors will most probably be in use in the forthcoming decades, due

to their low costs. Hydrodynamics are very important for the design and operation of the TBR reactors (**Calis et al., 2001**).The behavior of industrial reactor is significantly different from pilot plant reactors. While a pilot plant operates under ideal and isothermal state, the industrial reactor operates under non-isothermal state. Therefore, the dimensions of industrial trickle bed reactor should be addressed and the energy balance must be included in the mathematical model to evaluate the performance of an industrial trickle bed reactor for CWAO of phenol.

5.1. Energy Balance in Trickle Bed Reactor:

Most commercial trickle bed reactors normally operate adiabatically at high temperatures and high pressures. Kinetics and thermodynamics of reactions conducted in trickle bed reactors require high temperatures (**Al-Dahhan et al., 1997**). Reactions carried out in trickle bed reactors such as hydrogenation and oxidation can be highly exothermic. Although a lot of studies were carried out in the last thirty years in the field of trickle bed reactors, most of them have ignored the heat transfer. Furthermore, a major part of the heat transfer studies in trickle bed reactors have been carried out with water and air (or nitrogen) (**Lamine et al., 1996**). Temperature distribution in trickle bed reactors plays avery important role in designing and analyzing such reactors.

Average reactor temperature would always increase along the catalyst bed. For predicting the real performance of the industrial trickle bed reactors using the experimental information from small reactors, it is essential to add the heat balance equation in a commercial reactor model (**Mederos et al., 2009**). Non-isothermal behavior along the catalyst bed inside industrial trickle bed reactor can be described by a heat balance equation (**Rodriguez and Ancheyta, 2004; Mederos and Ancheyta, 2007**) as:

$$\frac{dT}{dz} = (-\Delta H_{r,T}) R_{ph} \rho_B \frac{\varepsilon_l}{u_g \rho_g cp^{O2} \varepsilon_{gg} + u_l \rho_L cp^{L} \varepsilon_L} \quad \textbf{(41)}$$

The heat capacity of liquid phenol (cp^{ph}) and gas oxygen (cp^{O2}) are calculated as a function temperature by the following relations (**John and Smith, 2007**).

$$cp^{ph} = 4.403 + 0.36338 \times T - 6.0417 \times 10^{-5} \times T^2 - 1.279 \times 10^{-7} \times T^3 \quad \textbf{(42)}$$

$$cp^{O2} = 30.255 + 0.00421 \times T - 188728 / T^2 \quad \textbf{(43)}$$

Within the reactor, the gas phase fraction (ε_{gg}) is determined based on bed void fraction and liquid phase fraction as shown below (**Mederos et al., 2009**):

$$\varepsilon_{gg} = \epsilon_B - \varepsilon_l \quad \textbf{(44)}$$

The heat of reaction ($\Delta H_{r,T}$) of phenol oxidation (Equation 45) is calculated (**John and Smith, 2007**) using Equation (46):

$$C_6H_5OH + 7O_2 \rightarrow 6CO_2 + 3H_2O \quad \textbf{(45)}$$

$$\Delta H_{r,T} = \Delta Hr^{\circ}_{298} + R \int_{T_0}^{T} \frac{\Delta cp^{\circ}}{R} dT \quad \textbf{(46)}$$

The heat of reaction at standard temperature can be calculated as:

$$\Delta Hr^{\circ}_{298} = \sum v_i \Delta Hfi^{\circ}_P - \sum v_i \Delta Hfi^{\circ}_R \quad \textbf{(47)}$$

v_i: Stoichiometric coefficient for reactant and product in chemical reaction equation, which is negative for reactant, and positive for product.

The standards heat of formation for each component, are listed in Table (3) (**John and Smith, 2007**)

The second term of equation 46 can be calculated as follows:

$$R\left(\int_{T_0}^{T} \frac{\Delta cp^{\circ}}{R}\, dT\right)=R\left((\Delta A(T-T_0)+\frac{\Delta B}{2}(T^2-T_0^2)+\frac{\Delta C}{3}(T^3T^3)\frac{\Delta D}{1}(\frac{T-T_0}{T\,T_0})\right) \quad \textbf{(48)}$$

$$\Delta A=\sum v_i A_i \quad \textbf{(49)}$$

$$\Delta B=\sum v_i B_i \quad \textbf{(50)}$$

$$\Delta C=\sum v_i C_i \quad \textbf{(51)}$$

$$\Delta D=\sum v_i D_i \quad \textbf{(52)}$$

A_i, B_i, C_i, and D_i are constant values in heat capacities equation. Solving the equations 41 to 52 give temperature profile as shown in Figure (3).

5.2. Reactor Dimension - Optimal Ratio of $\frac{L_r}{D_r}$

The radial concentration gradient that represents the degree of flow mixing occurring during the residence time in reactor can effect the mass velocity or conversion. Since radial dispersion tend to reduce the conversion and it is necessary to design these reactors with minimum effect of radial dispersion effect (**Mary et al., 2009**). To ensure the effect of radial concentration gradient as low as possible, it is necessary to find the optimal ratio of length to diameter of the reactor. The best common ratio of length to diameter lies approximately between 2 to 3**(Rodriguez and Ancheyta, 2004; Mederos and Ancheyta, 2007**).

An important criterion (based on the ratio of the bed length (L_r) to reactor diameter (D_r)) selected to neglect the radial dispersion that effects in packed bed reactor is as follow (**Bischoff and Levenspiel, 1962**):

$$\frac{L_r}{D_r} > 0.04\,\frac{u_l\,D_r}{\varepsilon_1\,D_r^L} \quad \textbf{(53)}$$

The liquid phase fraction (ε_1) can be estimated from the following correlation (**Cotta et al., 2000**):

$$\varepsilon_1 = 9.9\left(\frac{\rho_L u_L d_s}{\mu_L}\right)^{1/3}\left(\frac{d_s^3\, g\, \rho_L^2}{\mu_L^2}\right)^{-1/3} \quad \textbf{(54)}$$

The radial mass dispersion coefficient (D_r^L) can be calculated from the following equation (**Mederos and Ancheyta, 2007**):

$$D_r^L = \frac{d_p u_l}{\varepsilon_1\,P_e} \quad \textbf{(55)}$$

Peclet number (P_e) depends on the mode of operation and the type of the reactor (pilot plant or commercial reactor). For concurrent operation with a commercial unit, the Peclet number is estimated from the Sater-Levenspiel correlation as reported in (**Mederos and Ancheyta, 2007**) as follows:

$$P_e=7.58\times 10^{-3} Re_L^{0.703} \quad \textbf{(56)}$$

Re_L: Reynold number of liquid phase, which calculates as follow:

$$Re_L=\frac{\rho_L u_L d_p}{\mu_L} \quad \textbf{(57)}$$

Note, the capital cost of the reactor at the end dictates the dimension of the reactor. The capital cost (C_r,\$) of a reactor increases by increasing diameter and decreasing length of reactor which can be calculated using the following equation (assuming that the reactor is filled with the catalyst) (**Jarullah et al., 2012b**):

$$C_r(\$)=\left(\frac{M\ \&\ S}{280}\right)101.9\ D_r^{1.066}L_r^{0.802}(2.18+F_c) \quad \textbf{(58)}$$

$$F_c=F_m\ F_p \quad \textbf{(59)}$$

M & $S$is Marshal and Swift index for cost escalation (M & S= 1536.5) (**Sami et al., 2015**).

F_c,F_m and F_p are dimensionless factors that are function of the construction material and operating pressure (F_m=3.67, F_p=3.93) (**Jarullah et al., 2012d**).

5.2.1. Optimization Problem Formulation for Optimal Reactor Dimension

According to equation 53, let

$$a_2=\frac{L_r}{D_r} \quad \textbf{(60)}$$

$$b_2=0.04\ \frac{u_l\ d_p}{\varepsilon_1\ D_r^L} \quad \textbf{(61)}$$

$$ca_2=a_2-b_2 \quad \textbf{(62)}$$

$ca_2 > 0$

The optimization problem can be stated as:

Given	Phenol, catalyst, reaction temperature, oxygen partial pressure, LHSV and gas flow rate
Determine	Length of the reactor (L_r) and the diameter of the reactor (D_r)
So as to minimize	Capital cost of reactor (C_r)
Subjected to	Process constraints and linear bounds on all decision variables

Mathematically, the optimization problem can be written as:

Min C_r

L_r,D_r

s.t	f(x(z),u(z), v) = 0	(model equation, equality constraint)
	$ca_2 \geq 0$	(Inequality constraints)
	$L_r^L \leq L_r \leq L_r^U$	(Inequality constraints)
	$D_r^L \leq D_r \leq D_r^U$	(Inequality constraints)

5.3. Optimal Reactor Operating Conditions Based on Maximum Conversion and Minimum Cost

The phenol conversion depends on the operating conditions, hence it is necessary to find the optimal operating conditions that can give highest conversion with minimum cost. Many of the process variables can effect the phenol conversion and the cost of the process. Depending on the simulation results (presented in section 6),it has been noticed that the conversion of phenol increases with increasing temperature and decreasing liquid hourly space velocity, and this would result in higher operating costs due to the use of more utilities, oxygen, and catalyst. The cost function defined in equation 63 (**Hamad et al., 2005**) should be minimized to reduce the cost of the process with increasing production:

$$C_{FUNCTION.}=\left(\frac{C_{cat.}}{t_{cat.}} + C_{Oxy.} + C_{phen.} + C_{compression} + C_{pumping} + C_{Energy} - C_{conversion}\right) \quad \textbf{(63)}$$

$C_{FUNCTION}$, $C_{cat.}$, $C_{Oxy.}$,$C_{phen.}$,$C_{compression}$, $C_{pumping}$, C_{Energy} ,$C_{conversion}$, are function, catalyst, oxygen, phenol, compression, pumping, energy and conversion cost ($/yr), respectively. Each item of this equation is detailed below.

- **Catalyst Cost ($\boldsymbol{C_{cat}}$)**, ($/yr) can be calculated based on cycle life time ($t_{cat.}$) and price of catalyst as (10 yr) and 5.8$\frac{\$}{\text{kg}}$ (**www.epa.gov/tri**) respectively:

  $$\boldsymbol{C_{cat.}}(\$/\text{yr})= \left(V_{cat}(m^3)\right)\left(\rho_{cat}\left(\frac{kg}{m^3}\right)\right)\left(5.8\ (\frac{\$}{kg})\right)\left(\frac{1}{t_{cat}(yr)}\right) \quad \textbf{(64)}$$

- **Oxygen Cost ($C_{Oxy.}$),** ($/yr) can be estimated with a price of oxygen as 0.021$/kg, (**Estela and Mariano, 2015**)) using the following equation:

  $$C_{Oxy.}, (\$/\text{yr})=(\rho_{O2}(\text{kg/m}^3))\times(Q_{O2}(\text{m}^3/\text{sec}))\times(0.021(\$/\text{kg})\times 3600\times 24\times 3) \quad \textbf{(65)}$$

- **Phenol cost ($C_{phen.}$),** ($/yr) is evaluated based on the price of 1.58 ($/kg), (**Estela and Mariano, 2015**) as follows:

  $$C_{phen.},(\$/\text{yr})=(\ \rho_{\text{ph}}(\text{kg/m}^3)\times Q_{ph}(\text{m}^3/\text{sec.})\times(1.58(\$/\text{kg}))\times 3600\times 24\times 342) \quad \textbf{(66)}$$

- **Compression Cost ($\boldsymbol{C_{compression}}$),** ($/yr) can be calculated utilizing the following relationship based on the motor efficiency of 90% (**Bouton and Luyben, 2008**) and the average power price of 0.06$/kWh (**Estela and Mariano, 2015**):

  $$\boldsymbol{C_{comprision}}, (\$/\text{yr})=\left(\frac{bhp(hp)}{0.9}\right)\left(\frac{1kW}{1.341\ hp}\right)\left(\frac{o.o6\ \$}{kWh}\right)\left(\frac{24h}{1\ day}\right)\left(\frac{342}{1yr}\right) \quad \textbf{(67)}$$

  $$bhp= \frac{hp}{\eta_{ise}} \quad \textbf{(68)}$$

  $$hp= \left(\frac{3.03\times 10^{-5}}{\gamma}\right) P_{in}Q_{in}\left(\left(\frac{P_{out}}{P_{in}}\right)^{\gamma}-1\right) \quad \textbf{(69)}$$

  $$\gamma= \frac{\left(\frac{cp^{O2}}{cv^{O2}}-1\right)}{\left(\frac{cp^{O2}}{cv^{O2}}\right)} \quad \textbf{(70)}$$

  $$cv^{O2}= cp^{O2}-R \quad \textbf{(71)}$$

η_{ise}: Isentropic efficiency, reported to be from 70 to 90%. Here, it is assumed 90% (**Douglas, 1988; Bouton and Luyben, 2008**).

- **Pumping Cost ($C_{Pumping}$)**, ($/yr) can be estimated using the following relationship:

$$C_{pumping} = \left(Q_p(kW)\right)\left(\frac{0.06\ \$}{kWh}\right)\left(\frac{24h}{1\ day}\right)\left(\frac{342}{1yr}\right) \quad \textbf{(72)}$$

- **Energy Cost (C_{Energy})**, ($/yr), is calculated by using the following relation:

$$C_{Energy} = \beta \times (Q_{ph} + Q_{O2})\ (\mathrm{m^3/sec}) \times (3600 \times 24 \times 342)(T_{req} - 298) \quad \textbf{(73)}$$

β: Energy factor, 5.68×10^{-3} ($/m^3.℃), (**Hamad et al., 2005**).

- **Conversion Cost ($C_{conversion}$)**, ($/yr) can be estimated as follow:

$$C_{conversion} = C_{factor}(\$/\mathrm{m^3}) \times Q_{ph}(\mathrm{m^3/sec}) \times (3600 \times 24 \times 342) \quad \textbf{(74)}$$

The conversion factor (C_{factor}) can be considered the difference between the price of the product and the feed. This value has been assumed to be exponential with respect to the conversion as described in the following equation (**Hamad et al., 2005**):

$$C_{factor} = S_1 \exp(S_2 \times X_{ph}) \quad \textbf{(75)}$$

S_1 and S_2 are constant parameters of the conversion cost factor.

X_{ph}: Conversion of phenol

$$X_{ph} = \frac{C_{ph,0} - C_{ph}}{C_{ph,0}} \quad \textbf{(76)}$$

The cost factor is quantified in Figure (4) for different values of S_1 and S_2. The values of these parameters are based on the assumption that the benefit of extra conversion is directly related to the cost of the catalyst and the energy requirement. The values obtained by the simulation and optimization runs are S_1= 400.54 and S_2= 0.653 depending on the range of the catalyst cost from 630 to 780 $\$/m^3$ as shown in the Figure (4).

5.3.1. Optimization Problem Formulation for Optimal Operation

The optimization problem can be stated as:

Given	Length of the reactor (L_r), the diameter of the reactor (D_r) and reaction orders of phenol and oxygen (n and m).
Determine	Phenol, catalyst, and oxygen cost, reaction temperature, oxygen partial pressure, LHSV, initial phenol concentration and gas flow rate.
So as to minimize	Cost Function ($C_{FUNCTION.}$)
Subjected to	Process constraints and linear bounds on all decision variables

Mathematically, the optimization problem can be written as:

Min $C_{FUNCTION.}$

LHSV, S.E., P, T_R, $C_{ph,0}$

s.*t* f(x(z), u(z), v) = 0 (model equation, equality constraint)

$LHSV_r^L \leq LHSV_r \leq LHSV_r^U$ (Inequality constraints)

$S.E^L. \leq S.E. \leq S.E.^U$ (Inequality constraints)

$P^L \leq P \leq P^U$ (Inequality constraints)

$T_R{}^L \leq T_R \leq T_R{}^U$ (Inequality constraints)

$X_{ph}^L \leq X_{ph} \leq X_{ph}^U$ (Inequality constraints)

$C_{FUNCTION.} \geq 0$ (Inequality constraints)

6. Results and Discussions

6.1. The Best Kinetic Parameters of the Model (Based on Pilot Plant Experiment)

The values of constant parameters used in the mathematical model are given in Table (4). As described earlier, the model kinetic parameters of CWAO of phenol are estimated using two approaches.

In the first approach, the reaction orders of phenol concentration (*n*)and oxygen partial pressure (*m*) and reaction rate constants (K_{het}) at each temperature were estimated separately, then activation energy and pre-exponential factor are estimating by linearization of Arrhenius equation shown in equation (77) and equation (78). Figure (5) shows the linearization method by a plot (lnK_{het}) vs. (1/T) gives a slope (-EA/R) and intercept ($\ln A^0$). The kinetic parameters that estimated in this method are listed in Table (5).

$$K_{het} = A^0 \exp\left(-\frac{EA}{RT}\right) \quad \textbf{(77)}$$

Linearization of equation (77) will result in the following equation:

$$Ln(K_{het}) = Ln(A^0) - \left(\frac{EA}{R}\right)\frac{1}{T} \quad \textbf{(78)}$$

In the second approach, activation energy (*EA*), pre-exponential factor (A^0) and reactions order of phenol concentration (n) and oxygen partial pressure (m) were determined simultaneously and presented in Table (8). The parameter estimation from the second approach is more accurate than that calculated from the first approach, because the second approach gives smaller *SSE* than the first approach. However, the values of the activation energy (EA) and pre-exponential factor (A^0) that estimated via linearization (first approach) of Arrhenius equation gives high error as compared with those estimated via non-linear method (second approach).

Many researchers have studied the CWAO of phenol in aqueous wastewater, as reported in literatures. However, the optimal value of the order of phenol concentration (*n*) is (2.1066) as mentioned above. Different values of phenol concentration have been reported in literature as a first order (**Liu et al., 2008; Albin et al., 1997; Qinglin and Karl, 1998; Fortuny et al., 1999; Christoskova and Stoyanova, 2001; Wadood and Sama, 2008),** 1.5 (**Santos et al., 2005**) and 2 to 2.2 (**Safaa, 2009; Oscar et al., 2007**).

Optimal value of the order of the partial pressure (m) has been estimated to be (0.6111), several values have been reported in literatures as, zero order (**Christoskova and Stoyanova, 2001**), or 0.5 ($\pm$ 0.1) (**Safaa, 2009; Albin et al., 1997; Fortuny et al., 1999; Wadood and Sama, 2008).**

Also the values of the activation energy (EA) and pre-exponential factor (A^0) has been estimated by the second approach to be 16315.735 J/mole and (668879.2 sec^{-1} $(cm^3/mole)^{-1.11}$), respectively. A wide range of values of activation energy and pre-exponential factor have been reported in the public domain as 53000 J/mol (**Qinglin and Karl, 1998**), 55880 J/mol (**Christoskova and Stoyanova, 2001**), 61000 J/mole (**Albin et al., 1997**) and 75000 ($\pm$3) J/mol (**Fortuny et al., 1999**), 78500 J/mole (**Wadood and Sama, 2008)**,while the values of pre-exponential factor have been reported in literatures to be $1.3 \times 10^9(\pm 1 \times 10^8)$ $h^{-1}bar^{-1/2}$ (**Fortuny et al., 1999**), 3.2 ×1011 L/kg_{Cat}.h. (**Wadood and Sama, 2008**), which gives a clear indication that the values obtained in this study were within the range reported in the public domain.

In order to be sure about precision of the evaluated kinetic parameters, sensitivity analysis for *n, m, EA* and A^0 values is performed. Sensitivity analysis is utilized to each of the estimated parameters by means of perturbations of the parameter value and is preferably in the range of ±10%, keeping the other parameters in their evaluated values (**Jarullah et al., 2011a**). For each perturbation in the parameter values, the objective function is re-evaluated and then for each parameter the perturbation percentage is plotted against the corresponding value of the objective function as shown in Figure 6 (for each parameter). The global minimum is achieved when all the perturbations in all the kinetic parameters give the same minimum of the objective function with their original values (0% perturbation). In other words, poor nonlinear parameter estimation can be found if at least one parameter does not give the same minimum than the others at 0% perturbation. From Figure 6, it is clearly seen that the evaluated kinetic parameters are the optimum since at 0% perturbation the perturbations of *n, m, EA* and A^0give the same minimum of the objective function (SSE) with their original values. Therefore, it is demonstrated that the global minimum has been achieved. It has also been observed from Figure 6, *n* has the greatest effect on CWAO kinetic model compared to *EA, m*, and A^0, respectively.

6.2. Effect of Different Variables on Phenol Conversion

The TBR process model with the best kinetics parameters reported in section 6.1 is now simulated by varying different process operating parameters to gain deeper insight of the process.

6.2.1. Effect of Temperature

Figure (7a) shows that at temperature of 120℃ and LHSV of 1 hr^{-1}, the conversion of phenol is 87.954% and increasing the temperature to 140℃or160℃ at the same liquid hourly space velocity, results in higher conversions of phenol (90.878% and 93.13% respectively). This behavior can also be introduced in Figures (7b,c) at LHSV of 2 and 3 hr^{-1}. From these Figures (7a,b,c), it is observed that a good agreement between the predicted and experimental results. Higher conversion of phenol obtained at higher temperature can be attributed to the fact that the reaction rate constant is a function of reaction temperature (directly proportional) and activation energy (inversely proportional). Also rising temperatures can lead to the formation of free oxygen radicals ($O^{\cdot}$), which can react with oxygen and water to form H_2O_2 andO_3. These species are all capable in participating in the oxidation of phenol. It is important to understand the link between the temperature and the catalyst deactivation. Increased temperature renders the possibility of coke formation and pores blockage making rapid catalyst deactivation.. Therefore, it is necessary to determine the applicable range of temperature used. The results presented in this section are in agreement with

Qinglin and Karl (1998), Fortuny et al. (1999), Santos et al. (2005), Ayude et al. (2007), Wadood and Sama (2008) and Wadood (2014).

6.2.2. Effect of Liquid Hourly Space Velocity

The influence of liquid hourly space velocity (LHSV) on the phenol conversion was studied in the range (1, 2 and $3hr^{-1}$) with keeping other parameters constant (oxygen partial pressure = 0.8, initial phenol concentration = $5gm/l$, and gas flow rate =80%). The comparison between the experimental and the predicted results are plotted in Figures (8a,b,c).

As shown in these Figures, an increase in liquid hourly space velocity causes a decrease in phenol conversion. The conversion of phenol at 120℃ is 87.954 % was achieved at LHSV=$1hr^{-1}$, whereas the conversions of phenol decreased up to 73.12% and 59.18% at LHSV of 2 and $3hr^{-1}$ respectively as noted in Figure (8a). The same behavior has also been observed in Figures (8b,c). Furthermore, based on the results obtained in these Figures, a very well agreement between the predicted and experimental results has been observed.

The behaviors presented above are attributed to the following reasons: increasing liquid hourly space velocity means reducing residence time of reactants in the reactor leading to decrease in phenol conversion and vice versa. These results are in agreement with **Fortuny et al. (1999), Eftaxias et al. (2001), Ayude et al. (2007) and Wadood (2014**).

6.2.3. Effect of Oxygen Partial Pressure

The influence of oxygen partial pressure was studied in the range of 0.8, 1 and 1.2 MPa with constant temperature of 160℃, Initial phenol concentration of $5gm/l$, and gas flow rate of 80%. The comparison between the experimental and predicted data is plotted in Figure (9).

As can be seen from Figure (9), increasing oxygen partial pressure from 0.8 to 1.2 MPa the phenol conversion increased from 93 to 94.6% and the results showed a good agreement between the experimental and the predicted results with maximum average absolute error less than 5%. The oxygen partial pressure compared to temperature has a significant impact on the phenol conversion. Generally, increasing oxygen partial causes increasing phenol conversion due to increasing density and solubility of the gas. These results were agreement with the behavior published in the literature (**Fortuny et al., 1999; Ayude et al., 2007; Wadood and Sama, 2008; Wadood, 2014).**

6.2.4. Effect of Initial Phenol Concentration

The impact of initial concentration on the phenol conversion was studied in the range (1, 3 and $5gm/l$), with keeping others parameters constant (temperature= 160℃, oxygen partial pressure= 0.8 MPa and gas flow rate = 80%). The comparison between the experimental and the predicted data is plotted in Figure (10) and a good agreement between the predicted and the experimental results have been obtained

It is noted from Figure (10) that the phenol conversion increased with increasing initial phenol concentration from 80.35% to 94.75% at 1 and $5gm/l$ (initial phenol concentration), respectively owning to the increasing phenol molecules that cover the active sites of catalyst.

The results presented in this section were in agreement with the results reported in the public domain (**Christoskova and Stoyanova, 2001; Oscar et al., 2007; Ayude et al., 2007**).

6.2.5. Effect of Gas Flow Rates

The influence of gas flow rate (meaning stoichiometric excess, S.E. %) on the phenol conversion are studied in the range (20, 40, 80 and 100%) at different liquid hourly space velocity, where the other parameters are kept constant (temperature =140℃, oxygen partial pressure = 0.8 MPa and initial phenol concentration = $5gm/l$). The experimental and the predicted results are plotted in Figures (11a,b,c,d).

It is observed from Figures (11a) that the phenol conversion is 89 % at 20% gas flow rate and $1hr^{-1}$. Increasing the gas flow rate increases the conversion of phenol. The highest conversion (91.5%) is obtained at gas flow rate of 80%. It is also observed that an increase in gas flow rate causes an increase in the liquid hold up as well as the liquid film thickness covered catalyst surface, thus enhancing oxygen transfer to the liquid phase and from the liquid phase to the catalyst surface leading to high conversion. However, increasing the gas flow rate up to 100% causes slightly decrease in the phenol conversion because of decreasing spread of the liquid film over the catalyst. Hence, wetting was decreased. These results are in agreement with the results published in the literature (**Fortuny, et al., 1999; Eftaxia, et al., 2001; Wadood, 2014**).

6.3. Case 2: Optimal Ratio of L_r/D_r

The capital cost of reactor (C_r,\$) depends on $\frac{L_r}{D_r}$ ratio (in terms ofa_2). Where, the capital cost of the reactor increases with increasing diameter and decreasing length of the reactor. Also, the radial dispersion can affect the process performance but is related to the ratio of length to diameter of the reactor. In such case to avoid the effect of radial dispersion and to obtain high conversion with minimum cost, optimal values of a_2 and $b_2$with the capital cost of reactor are calculated and optimized and are presented in Table (7).

However, to ensure safe operation and in order to avoid any side effect of the radial dispersion, 5 % is added on $\frac{L_r}{D_r}$ratio. Thus, the simulation results with the final dimensions of the reactor are shown in Table (8).

6.4. Optimal Operating Conditions Based on Maximum Conversion and Minimum Cost

Based on the optimal reactor dimension, it is necessary to obtain the optimal values of the operating conditions which can affect the efficiency of the process, such as the conversion and the productivity. The optimal values of the best operating conditions used in CWAO process operation conditions are presented in Table (9).

From this Table, it is observed that the effect of temperature having the biggest impact on the CWAO process compared with others operating conditions. The optimum temperature of 472.87 K gives the maximum conversion of 99.79 % with minimum cost of 190507980 \$/yr. On the other hand, gas flow rate needs to be about 20 % that has less effect compared to temperature influence to have such conversion.

The cost parameters obtained by the optimization process are listed in Tables (10). As can be seen from this Table, the biggest effect of the cost function of the CWAO process can be attributed to the energy cost as opposed to the operating cost and the energy cost is related to the phenol conversion and temperature as well.

7. Conclusions

- Design of industrial trickle bed reactor with the optimal operation of commercial catalytic wet air oxidation (CWAO) of phenol is studied for evaluating viability of large-scale operation of phenol oxidation process. The mathematical model has been developed using a Langmuir-Hinshelwood formulation to predict the performance of oxidation kinetic phenol in a trickle bed reactor employing pure oxygen as an oxidant and catalyst (pt/γ-Al_2O_3) under different operating conditions temperature 120, 140 and 160℃, oxygen partial

pressure 0.8, 1 and 1.2 MPa, liquid hourly space velocity(1, 2, and 3hr^{-1}), initial phenol concentration (1, 3, and 5gm/l), and gas flow rate(stoichiometric excess) (20, 40, 80 and 100%).

- The best kinetic parameters of this model were estimated via optimization technique using two approaches (Linear& Non-Linear methods) based on experimental results. It is found that the second approach (Non-Linear method) is more accurate based on minimizing the sum of squared error between experimental and predicted results with average absolute error les that 5% among all the results at various conditions.
- Optimal ratio of reactor bed length to the reactor diameter (L_r/D_r) has been taken into account in the case of scaling up to minimize the effect of radial dispersion. It can be concluded that the decrease in L_r/D_r ratio leads to increasing hydrodynamic effects with decreasing the capital cost of the reactor and the optimal ratio was found to agree well with the limitation reported in the literature and the optimized value within gPROMS program is 3.265 to get safe operation and preventing any side effects.
- The conversion of phenol depends on the process conditions, thus the optimal operating conditions (mainly, T, P, LHSV, S.E. Initial concentration of phenol) that can be effectively used to reactor design and operation have also been investigated here to get the maximum conversion of phenol based on the minimum cost of the process. The maximum conversion of phenol (99.79%) with minimum cost for the industrial CWAO process is obtained at 472.87K, 0.6 bar, 0.5 hr^{-1}, 20% and 1.0498×10^{-5}mol/cm^3 for T, P, LHSV, S.E. Initial concentration of phenol, respectively.

Nomenclature

a_{GL}	Specific gas-liquid contact area per unit volume of bed	cm^{-1}
a_{LS}	Specific liquid–solid contact area per unit volume of bed	cm^{-1}
A^0	Pre-exponential factor	$(mole/cm^3)^{1-n}.sec^{-1}$
$BO^l_{a,m}$	Bodenstein number for liquid phase	*(-)*
C_{Energy}	Energy cost	*$/yr*
$C_{FUNCTION}$	Function cost	*$/yr*
$C_{O2,G}$	Concentration of oxygen in gas phase	mol/cm^3
$C_{O2,L-s}$	Concentration of oxygen at liquid–solid Interface	mol/cm^3
$c_{O2,L}$	Concentration of oxygen in liquid phase	mol/cm^3
cp^{O2}	Heat capacity of oxygen	*J/mole. K*
cp^{ph}	Heat capacity of phenol	*J/mole. K*
cv^{O2}	Specific heat capacity for oxygen at constant volume	*J/mole. K*
$C_{Oxy.}$	Oxygen cost	*$/yr*
$C_{cat.}$	Catalyst cost	*$/yr*
$C_{compression}$	Compression cost	*$/yr*
$C_{conversion}$	Conversion cost	*$/yr*

$C_{ph,0}$	Initial concentration of phenol	*mol/cm^3*
$C_{ph,L-s}$	Concentration of phenol at liquid-solid interface	*mol/cm^3*
$C_{ph,L}$	Concentration of phenol in liquid phase	*mol/cm^3*
C_{ph}	Concentration of phenol	*mol/cm^3*
$C_{phen.}$	Phenol cost	*$/yr*
$C_{pumping}$	Pumping cost	*$/yr*
d_t	Tube diameter	*cm*
d_P	Diameter of catalyst particle	*cm*
dp_e	Equivalent diameter particle of catalyst	*cm*
D_a^l	Over all axial dispersion coefficient	*cm^2/sec*
D_{O2}^L	Molecular diffusivity of oxygen in liquid phase	*cm^2/sec*
D_{ei}	Effective diffusivity	*cm^2/sec*
D_{ph}^L	Molecular diffusivity of phenol in liquid phase	*cm^2/sec*
D_r	Rector diameter	*cm*
D_r^L	Radial mass dispersion coefficient	*cm^2/sec*
Ga_l	Galaleo number of liquid phase	*(-)*
EA	Activation energy	*J/mole. K*
H_{O2}	Henry's law constant for dissolved oxygen in water	*(-)*
K_{het}	Apparent reaction rate constant	*(mole/cm^3)$^{1-n}$.sec^{-1}*
k_{GL}	Gas-to-liquid mass transfer coefficient	*cm/sec*
k_{LS}	Liquid-to-solid mass transfer coefficient	*cm/sec*
K_{ph}	Adsorption equilibrium constant of phenol	*cm^3/sec*
L_r	Bed length of reactor	*cm*
M & *S*	Marshal and Swift index for cost escalation	*(-)*
m	Order of oxygen partial pressure	*(-)*
Mw_i	Molecular weight	*gm/gmol or lb/lbmol*
n	Order of phenol concentration	*(-)*
P	Partial pressure of oxygen	*bar*
P_c	Critical pressure of phenol	*psia*
P_e	Peclet number	*(-)*
P_{in}	Pressure inlet to the compressor	*lb/ft^2*
P_{out}	Pressure outlet of compressor	*lb/ft^2*
Q_{in}	Volumetric flowrate at compressor section	*ft^3/min*

Q_p	Pump power	*KW*
r_P	Radius of catalyst particle	*cm*
r_g	Mean pore radius	*cm*
Re_l	Reynold number of liquid phase	*(-)*
R_{ph}	Rate disappearance of phenol per unit volume of catalyst	$mole/cm^3_{cat}.sec$
S_g	Specific surface area of particle	cm^2/gm
S_P	Total geometric surface area of catalyst	cm^2
T_b	Boiling point temperature of phenol	℃
T_{br}	Reduced boiling point temperature	*(-)*
T_c	Critical temperature of phenol	R°
T_r	Reduced temperature which	*(-)*
$T_{req.}$	Required temperature to achieve required conversion	*K*
u_g	Superficial gas velocity	*cm/sec*
u_l	Superficial liquid velocity	*cm/sec*
V_P	Total geometric volume of catalyst particle	cm^3
V_g	Total pore volume	cm^3/gm
z	Length of catalyst bed	*cm*
Z_{O2}	Compressibility factor	*(-)*
Z_c	Critical compressibility factor	*(-)*

Greek letters

η_0	Effectiveness factor	*(-)*
η_{LS}	Wetting efficiency	*(-)*
ε_B	Bed void fraction (Bed porosity)	*(-)*
v_L	Molar volume of liquid	$cm^3/gmole$
v_{O2}	Molar volume of oxygen	$cm^3/gmole$
v_{ph}	Molar volume of phenol	$cm^3/gmole$
$\Delta H_{r,T}$	Heat of reaction at any temperature	*J/mole*
ΔHr°_{298}	Heat of reaction at standard temperature (298K)	*J/mole. K*
$\mu_{ph,b}$	Viscosity at boiling point	*mPa. Sec*
μ_{ph}	Viscosity of phenol	$gm/cm.sec$ *mPa. Sec*
ρ_{O2}	Density of oxygen	gm/cm^3

ρ_{cat}	Catalyst density	gm/cm^3
ρ_p	Particle density	gm/cm^3
ρ_{ph}	Density of phenol	gm/cm^3
ϵ_B	Bed porosity	*(-)*
$\emptyset$	Volume fraction of molecule	*(-)*
φ	Thiel Modulus	*(-)*
β	Energy factor	$\$/m^3.℃$
γ	Specific heat ratio	*(-)*

References

[1]. Albin, P., Gorazd, B., Janez, L. (1997). Catalytic liquid-phase oxidation of aqueous phenol solutions in a trickle-bed reactor. Chem. Eng. Sci., 36, 4143–4153.

[2]. Al-Dahhan, M.H., Faical, L., Milorad, P. Dudukovic, A.L. (1997). High pressure trickle bed reactors: A review. Ind. Eng. Chem. Res, 36, 3292–3314.

[3]. Ayude, A., Rodriguez, T., Font, J., Fortuny, A., Bengoa, C., Fabregat, A., Stüber, F. (2007). Effect of gas feed flow and gas composition modulation on activated carbon performance in phenol wet air oxidation. Chem. Eng. Sci., 62, 7351–7358.

[4]. Bhaskar, M., Valavarasu, G., Meenakshisundaram, A., Balaraman, K.S. (2002). Application of a three phase heterogeneous model to analyse the performance of a pilot plant trickle bed reactor. Petro. Sci. Tech., 20, 251–266.

[5]. Bischoff, K.B., Levenspiel, O. (1962). Fluid dispersion-generalization and comparison of mathematical models-II comparison of models. Chem. Eng. Sci., 17, 257–266.

[6]. Bouton, G.R., Luyben, W.L. (2008). Optimum economic design and control of a gas permeation membrane coupled with the hydrotreating (HAD) Process. Ind. Eng. Chem. Res., 47, 1221–1266.

[7]. Bruce, E.P., Jhon, M.P., Jhon, P.O. (2004). The Properties of Gases and Liquids. New York, McGraw-Hill.

[8]. Budavari, S. (1996). The Merck Index: An Encyclopedia of Chemical, Drugs and Biologicals. Whitehouse Station, NJ: Merck.

[9]. Busca, G., Berardinelli, S., Resini, C. Arrighi, L. (2008). Review-Technologies for the removal of phenol from fluid streams: A short review of recent developments. Journal of Hazardous Materials, 160, 265–288.

[10]. Calis, H.P.A., Nijenhuis, J., Paikert, B.C., Dautzenberg, .F.M., van den Bleek. C.M. (2001). CFD modelling and experimental validation of pressure drop and flow profile in a novel structured catalytic reactor packing. Chem. Eng. Sci., 56, 1713–1720.

[11]. Christoskova, S., Stoyanova, M. (2000). Degradation of phenolic waste waters over Ni-oxide. Water Research, 35, 2073 – 2077.

[12]. Cotta, R.M., Wolf-Maciel, M.R., Filho, R.M. (2000). A cape of HDT industrial reactor for middle distillates. Comp. and Chem. Eng., 24, 173–188.

[13]. Douglas, J.M. (1988). Conceptual Design Chemical Processes. New York, McGraw-Hill.

[14]. Dudukovic, M.P., Larachi, F., Mills, P.L. (2002). Multiphase catalytic reactors: a perspective on current knowledge and future trends. Catal. Rev. Sci. Eng., 44, 123–246.

[15]. Eftaxias, A., Fonta, J., Fortuny, A., Giralt, J., Fabregat, A., Stüber, F. (2001). Kinetic modelling of catalytic wet air oxidation of phenol by simulated annealing. Appl. Catal. B: Environ., 33, 175–190.

[16]. Estela, P., Mariano, M. (2015). Optimal production of dimethyl ether from switchgrass-based syngas via direct synthesis. Ind. Eng. Chem. Res., 54, 7465−7475.

[17]. Feike, J.L., Toride, N. (1998). Analytical solutions for solute transport with binary and ternary exchange. Soil Sci. Soc. Am. J, 56, 855–864.

[18]. Fortuny, A., Bengoa, C., Font, J., Castells, A., Fabregat, A. (1999). Water pollution abatement by catalytic wet air oxidation in a trickle bed reactor. Catal. Tod. 53, 107–114**.**

[19]. Fortuny, A., Font, J., Fabregat, A. (1998). Wet air oxidation of phenol using active carbon as catalyst. Appl. Catal. B: Environ., 19, 165–173.

[20]. Froment, G.F., Bischoff, K.B. (1990). Chemical Reactor Analysis and Design. 2nd ed. New York, Wiley.

[21]. Gierman, H. (1988). Appl. Catal. 43, 277-280.

[22]. Hamad, A.H., Al-Adwani, Haitham M.S. Lababidi, Imad, M. Alatiqi, Faisal, S. Al-Dafferi. (2005). Optimization study of residuum hydrotreating processes. Kuwait University, 83, 105-120.

[23]. Haughey, D.P., Beveridge, G.S. (1969). Structural properties of packed beds–a review. Can. Jour. Chem. Eng., 47,130–140.

[24]. Jarullah, A.T. (2011). Kinetic modeling simulation and optimal operation of trickle bed reactor for hydrotreating of crude oil. PhD Thesis. University of Bradford.

[25]. Jarullah, A.T., Mujtaba, I.M., Alastair, S.W. (2011a). Kinetic parameter estimation and simulation of trickle-bed reactor for hydrodesulfurization of crude oil. Chem. Eng. Sci., 66, 859–871.

[26]. Jarullah, A.T., Mujtaba, I.M., Alastair, S.W. (2011b). Improvement of the Middle Distillate Yields during Crude Oil Hydrotreatment in a Trickle-Bed Reactor. Energy Fuels, 25, 773−781.

[27]. Jarullah, A.T., Mujtaba, I.M., Alastair, S.W. (2011c). Kinetic model development and simulation of simultaneous hydrodenitrogenation and hydrodemetallization of crude oil in trickle bed reactor. Fuel 90, 2165‑2181.

[28]. Jarullah, A.T., Mujtaba, I.M., Alastair, S.W. (2011d). Modelling and Optimization of Crude Oil Hydrotreating Process in Trickle Bed Reactor: Energy Consumption and Recovery Issues. Chemical Product and Process Modeling, 6: Iss. 2, Article 3.

[29]. Jarullah, A.T., Mujtaba, I.M., Alastair, S.W. (2011e). Enhancement of Productivity of Distillate Fractions by Crude Oil Hydrotreatment: Development of Kinetic Model for the Hydrotreating Process. Computer Aided Chemical Eng., 29, 261–265.

[30]. Jarullah, A.T., Mujtaba, I.M., Alastair, S.W. (2012a). Whole Crude Oil Hydrotreating from Small-Scale Laboratory Pilot Plant to Large-Scale trickle-Bed Reactor: Analysis of Operational Issues through Modeling. Energy and Fuels, 26, 629–641.

[31]. Jarullah, A.T., Mujtaba, I.M., Alastair, S.W. (2012b). Economic Analysis of an Industrial Refining Unit Applied for Hydrotreating of Crude Oil in Trickle Bed Reactor using gPROMS. Computer Aided Process Eng., 30, 625–656.

[32]. Jarullah, A.T., Shymaa, A.H., Zina A.H. (2013). Optimal Design of Ammonia Synthesis Reactor. Tikrit Journal of Eng. Sci., 20, 22-31.

[33]. Jarullah, A.T., Arkan J.H., Shymaa, A.H. (2015). Optimal Design of Industrial Reactor for Naphtha Thermal Cracking Process. Diyala Journal of Eng. Sci., 8, 139-161.

[34]. John, Smith, (2007). Introduction to chemical engineering thermodynamic. Fourth edition.

[35]. Jordan, W., Van Barneveld, H., Gerlich, O., Kleine-Boymann, M., Ullrich, J. (1991). Phenol. In: Ullmann's encyclopedia of industrial chemistry, 5th ed., VCH, Weinheim.

[36]. Keav, S., Martin, A., Barbier J., Duprez, D. (2010). Deactivation and reactivation of noble metal catalysts tested in the catalytic wet air oxidation of phenol. Catal. Tod. 151, 143–147.

[37]. Liu, G., Zhang, X., Wang, L., Zhang, S., Mi, Z. (2008). Unsteady-state operation of trickle-bed reactor for dicyclopentadiene hydrogenation. Chem. Eng. Sci., 36, 4991–5001.

[38]. Lamine, A.S., Gerth, L., Gall, H.L.E., wild, G. (1996). Heat transfer in a packed bed reactor with co-current down flow of a gas and a liquid. Chem. Eng. Sci., 52, 3813–3827.

[39]. Lin, T.M., Lee, S.S., Lai, C.S., Lin, S.D. (June 2006). "Phenol burn". Burns: Journal of the International Society for Burn Injuries 32 (4): 517–21. doi:10.1016/j.burns.2005.12.016. PMID 16621299.

[40]. Mangrulkar, P.A., Bansiwal, A.K., Rayalu, S.S. (2008). Adsorption of phenol and o-chlorophenol on surface altered fly ash based molecular sieves, Chem. Eng. J., 138, 73–77.

[41]. Marroquin, G., Ancheyta, J., Esteban, C. (2005). A batch reactor study to determine effectiveness factors of commercial HDS catalyst. Catal. Tod., 104, 70–80.

[42]. Mary, G., Chaouki, J., Luck, F. (2009). Trickle-Bed laboratory reactors for kinetic studies. Intern. Journ. of Chem. React. Eng., 7, 1–8.

[43]. Massa, P.A., Ayude, M.A., Fenoglio, R.J., Gonzalez, J.F. Haure, P.M. (2004). Catalyst systems for the oxidation of phenol in water. Latin American Applied Research, 34, 133-140.

[44]. Mederos, F.S., Ancheyta, J. (2007). Mathematical modeling and simulation of hydrotreating reactors: Cocurrent versus countercurrent operations. Appl. Catal. A: Gen., 332, 8–14.

[45]. Mederos, F.S., Rodrý´guez, M.A. Ancheyta, J., Arce, E. (2006). Dynamic modelling and simulation of catalytic hydrotreating reactors. Energy & Fuels, 20, 936–940.

[46]. Nawaf, A.T. (2015). Experimental and modelling study for desulfurization of light gas oil by catalytic wet air oxidation process. MSc. Thesis. University of Tikrit.

[47]. Nawaf, A.T., Saba A.G., Jarullah, A.T., Mujtaba, I.M., (2015a). Optimal Design of a Trickle Bed Reactor for Light Fuel Oxidative Desulfurization Based on Experiments and Modeling. Energy Fuels, 29, 3366−3376.

[48]. Nawaf, A.T., Jarullah, A.T., Saba A.G., Mujtaba, I.M., (2015b). Improvement of Fuel Quality by Oxidative Desulfurization: Design of Synthetic Catalyst for the Process. Fuel Process Technology, 138, 337−343.

[49]. Nawaf, A.T., Jarullah, A.T., Saba A.G., Mujtaba, I.M., (2015c). Development of Kinetic and Process Models for the Oxidative Desulfurization of Light Fuel, Using Experiments and the Parameter Estimation Technique. Ind. Eng. Chem. Res., 54, 12503−12515.

[50]. Oscar P., Marıa J., Rivero, Inmaculada, O., Angel, I. (2007). Mathematical modelling of phenol photooxidation: Kinetics of the process toxicity. Chem. Eng. Jour. 134, 23–28.

[51]. Pintar, A., Levec, J. (1992). Catalytic liquid-phase oxidation of refractory organics in wastewater. Chem. Eng. Sci., 47, 2395–2400.

[52]. Perry, R.H., Green, D.W. (1999). Perry's Chemical Engineers' Handbook. New York, McGraw-Hill.

[53]. Poyton, A.A., Varziri, M.S., McAuley, K.B., McLellan, P.J., Ramsay, J.O. (2006). Parameter estimation in continuous-time dynamic models using principal differential analysis. Comp. Chem. Eng., 30, 698–708.

[54]. Qiang, W., Xijun, H., Po, L., Yue, J., Feng, X., Chen, H., Zhang, S., Qiao. (2009). Modeling of a pilot-scale trickle bed reactor for the catalytic oxidation of phenol. Separation and Purification Tech. 67, 158-165.

[55]. Qinglin, Z., Karl, T.C. (1998). Kinetics of wet oxidation of black liquor over a Pt-Pd-Ce/alumina catalyst. Appl. Catal. B: Environ., 17, 321–332.

[56]. Rackett H.G. (1970). Equation of State for Saturated Liquids. J. Chem. Eng. Data, 15, 514-517.

[57]. Reid, R.C., Prausnitz, J.M., Poling, B.E. (1987). The Properties of gases & liquids. 4th Ed. New York, McGraw-Hill.

[58]. Rodriguez, M.A., Ancheyta, J. (2004). Modeling of hydrodesulfurization (HDS), hydrodenitrogenation (HDN), and the hydrogenation of aromatics (HDA) in a vacuum gas oil hydrotreater. Energy & Fuels, 18, 789–790.

[59]. Safaa, M. (2009). Catalytic Wet Air Oxidation of phenolic compounds in wastewater in a trickle bed reactor at high pressure. MSc. Thesis. University of Tikrit.

[60]. Sameer A. E., Jarullah, A.T., Saba A.G. (2016). 5-Lumps kinetic modeling, simulation and optimization for hydrotreating of atmospheric crude oil residue. Appl. Petroleum Res., DOI 10.1007/s13203-015-0142-x.

[61]. Sami, M. Bahakim, Luis, A. Ricardez-Sandoval. (2015). Optimal design of a post combustion CO_2 capture pilot-scale plant under process uncertainty: A ranked-based approach. Ind. Eng. Chem. Res., 54, 3879-3892.

[62]. Santos, A., Yustos, P., Quintanilla, A., Ruiz, G. and Garcia-Ochoa, F.(2005). Study of the copper leaching in the wet oxidation of phenol with CuO-based catalysts: causes and effects, Appl. Catal. B: Environ. 61, 323–333.

[63]. Satterfield, C.N. (1975). Trickle-Bed Reactors. AIChE J, 21, 209-228.

[64]. Singh, A., Pant, K.K. and Nigam, K.D.P. (2004). Catalytic wet oxidation of phenol in a trickle bed reactor. Chem. Eng. J. 103, 51–57.

[65]. Vázquez, G., González-Álvarez, J., García, A.I., Freire M.S., Antorrena, G. (2007). Adsorption of phenol on formaldehyde-pretreated Pinus pinaster bark: equilibrium and kinetics. Bioresour. Technol., 98, 1535–1540.

[66]. Wadood, T.M., Sama, M.A., (2008). Kinetic Study on Catalytic Wet Air Oxidation of Phenol in a Trickle Bed Reactor. Jour. Eng. 9, 17-23.

[67]. Wadood T. M., (2014). Active Carbon from Date Stones for Phenol Oxidation in Trickle Bed Reactor, Experimental and Kinetic Study journal engineering, 9, 170-173.

List of Tables

List of Figures

Table 1: Specifications of experimental apparatus used in CWAO process (**Safaa, 2009**)

Parameters	Values
Length of reactor	77 cm
Length of the bed catalyst	30 cm
Inner diameter	1.9 cm
Volume of catalyst in bed	85 cm^3
Construction material	Stainless Steel

Table 2: Characterization of catalyst ($pt/\gamma - AL_2O_3$)

Specification	Values
Active phase	(0.48 wt%) pt
Support	$\gamma - AL_2O_3$
Calcination temperature	400 (ºC)
Pore volume	0.308 (cm^3/g)
Bulk density	0.647 (g/cm^3)
Surface area	259.9 (m^2/g)
Diameter Particle	1.6 *mm*
Particle shape	sphere

Table 3: Standards heat of formation the reactant and product component

Component	ΔHfi°, KJ/mole. K
C_6H_5OH	-172
O_2	0
CO_2	-393.509
H_2O	-241.818

Table 4: Values of constant parameters and coefficients used in this model

Parameter	Symbol	Unit	Value
Gas constant	R	J/mole. K	8.314
		$\frac{atm.\ lit.}{gmole.\ K}$	0.0823
		$\frac{ft^3.\ Psia}{Ibmole\ .\ R^{\circ}}$	10.73
Critical volume of liquid	$v_c{}^{L}$	$cm^3/gmole$	55.95
Critical volume of phenol	$v_c{}^{ph}$	$cm^3/gmole$	229
Critical volume of oxygen	$v_c{}^{O2}$	$cm^3/gmole$	73.4
Molecular weight of phenol	MW_{ph}	$gm/gmole$ $Ib/Ibmole$	94.11
Molecular weight of oxygen	MW_{O2}	$gm/gmole$ $Ib/Ibmole$	32
Critical temperature of phenol	T_c	R°	1250
Critical pressure of phenol	P_c	psia	901.11
Critical compressibility factor of phenol	Z_c	(-)	0.243
Compressibility factor of oxygen	Z_{O2}	(-)	0.2880
Catalyst bulk density	ρ_{cat}	gm/cm^3	0.647
Volume of catalyst	$V_{cat.}$	cm^3	85
Diameter of catalyst particle	d_p	cm	0.16
Catalyst bed length	Z	cm	30
Reactor diameter (Bed diameter)	D_r	cm	1.9
Total geometric volume of catalyst particle	V_P	cm^3	2.14×10^{-3}
Total geometric surface area of catalyst particle	S_P	cm^2	8.04×10^{-2}
Specific surface area of particle	S_g	cm^2/gm	2599000
Total pore volume	V_g	cm^3/gm	0.308

Table 5: Values of kinetic parameters obtained via first approach (Linear Method)

First Approach			
Parameter	**Symbol**	**Unit**	**Value**
Order of phenol concentration	*n*	(-)	2.1086
Order of oxygen partial pressure	*m*	(-)	0.6460
Apparent reaction rate constant @ 120℃	$K_{het.1}$	$sec.^{-1}\,(\frac{cm^3}{mole})^{-1.11}$	5440.644
Apparent reaction rate constant @140℃	$K_{het.2}$	$sec.^{-1}\,(\frac{cm^3}{mole})^{-1.11}$	6900.594
Apparent reaction rate constant @160℃	$K_{het.3}$	$sec.^{-1}\,(\frac{cm^3}{mole})^{-1.11}$	8690.253
Activation energy	*EA*	J/mole	16609.709
pre-exponential factor	A^0	$sec.^{-1}\,(\frac{cm^3}{mole})^{-1.11}$	874143.6496
Sum of Square Errors	*SSE*	(-)	5.4078E-4

Table 6: Values of kinetic parameters obtained via second approach (Non-Linear Method)

Second Approach			
Parameter	**Symbol**	**Unit**	**Value**
Order of phenol concentration	*n*	(-)	2.1066
Order of oxygen partial pressure	*m*	(-)	0.6112
Activation energy	*EA*	J/mole	16315.735
Pre-exponential factor	A^0	$sec.^{-1}\,(\frac{cm^3}{mole})^{-1.11}$	668879.2
Sum of Square Errors	*SSE*	(-)	4.8226E-4

Table 7: Optimal results between a_2 and b_2 with the capital cost (C_r,$)

Decision variable type	Optimal value
a_2	0
b_2	0
ca_2	0
L_r/D_r	3.265
L_r (cm)	878.9326
D_R (cm)	269.1983
C_r ($)	1715277.8

Table 8: Simulation results with addition 5 % on L_r/D_r ratio

Decision variable type	Simulation results
L_r/D_r	3.428
L_r (cm)	922.879
D_r (cm)	269.1983
C_r ($)	1801041.69

Table 9: Optimal operating conditions obtained for industrial CWAO process

Reaction Temperature	T_R	K	472.87
Partial Pressure of Oxygen	P	MPa	0.60
Liquid Hourly Space Velocity	$LHSV$	hr^{-1}	0.50
Gas Flow Rate (Stoichiometric Excess)	$S.E.$	-	0.20
Initial Phenol Concentration	$C_{ph,0}$	$mole/cm^3$	1.0498E-5

Table 10: Optimal values of the cost parameters used in this model

Cost Parameter	Symbol	Unit	Optimal Value
Oxygen Cost	$C_{Oxy.}$	$\$/yr$	39781.71
Phenol Cost	$C_{phen.}$	$\$/yr$	347559.32
Catalyst Cost	$C_{cat.}$	$\$/yr$	485251
Pumping Cost	$C_{pumping}$	$\$/yr$	68476
Compression Cost	$C_{comprision}$	$\$/yr$	43363
Energy Cost	C_{Energy}	$\$/yr$	469944.12
Conversion Cost	$C_{conversion}$	$/yr	155158210
Conversion	X_{ph}	$\%$	99.79
Cost Function	$C_{FUNCTION.}$	$\$/yr$	190507980

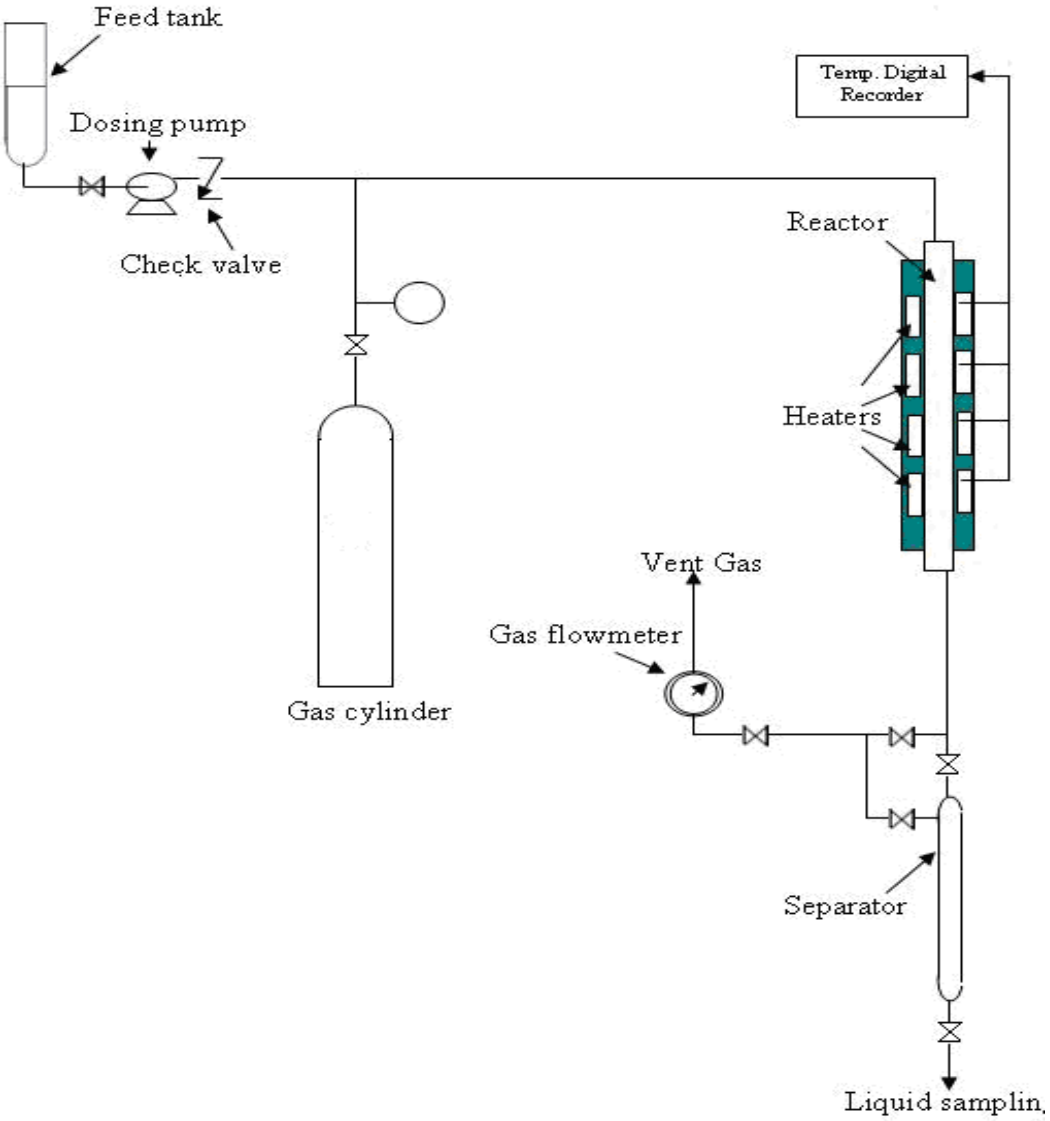
Feed tank
Dosing pump
Check valve
Temp. Digital Recorder
Reactor
Heaters
Vent Gas
Gas flowmeter
Gas cylinder
Separator
Liquid samplin

Figure 1

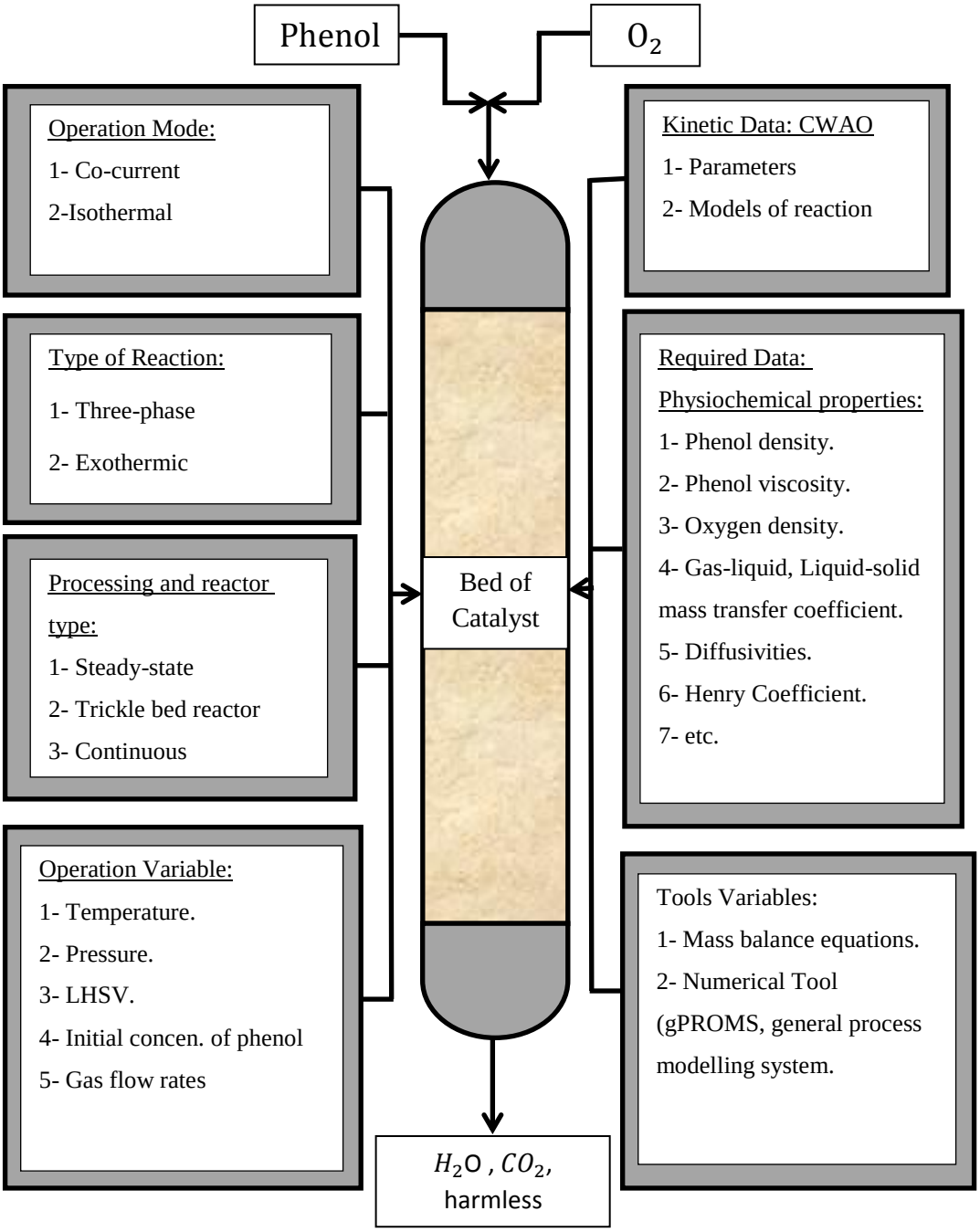
Phenol
O_2
Operation Mode:
1- Co-current
2-Isothermal
Kinetic Data: CWAO
1- Parameters
2- Models of reaction
Type of Reaction:
1- Three-phase
2- Exothermic
Required Data:
Physiochemical properties:
1- Phenol density.
2- Phenol viscosity.
3- Oxygen density.
4- Gas-liquid, Liquid-solid mass transfer coefficient.
5- Diffusivities.
6- Henry Coefficient.
7- etc.
Processing and reactor type:
1- Steady-state
2- Trickle bed reactor
3- Continuous
Bed of Catalyst
Operation Variable:
1- Temperature.
2- Pressure.
3- LHSV.
4- Initial concen. of phenol
5- Gas flow rates
Tools Variables:
1- Mass balance equations.
2- Numerical Tool (gPROMS, general process modelling system.
H_2O , CO_2, harmless

Figure 2

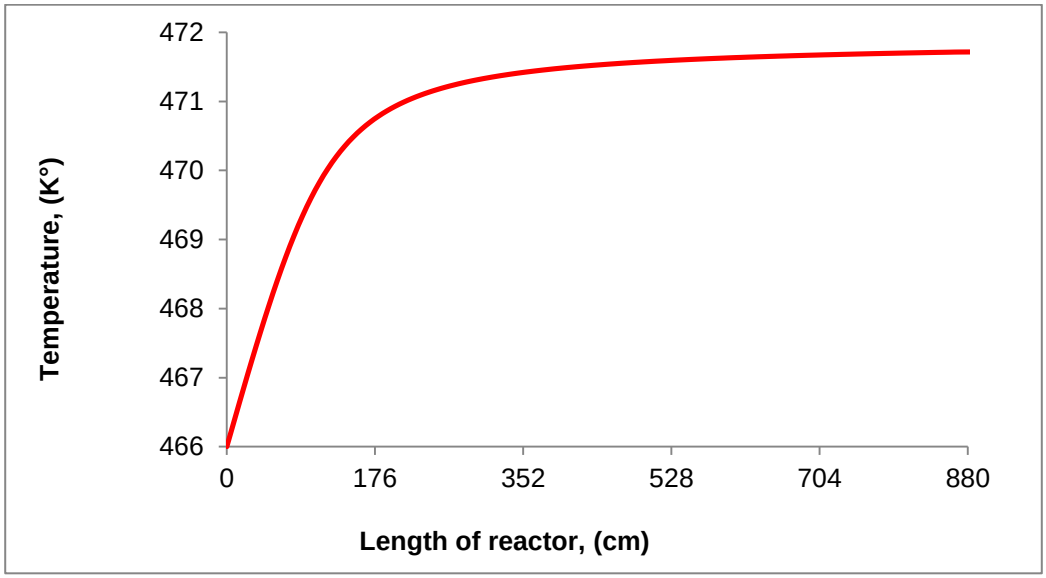

Figure 3

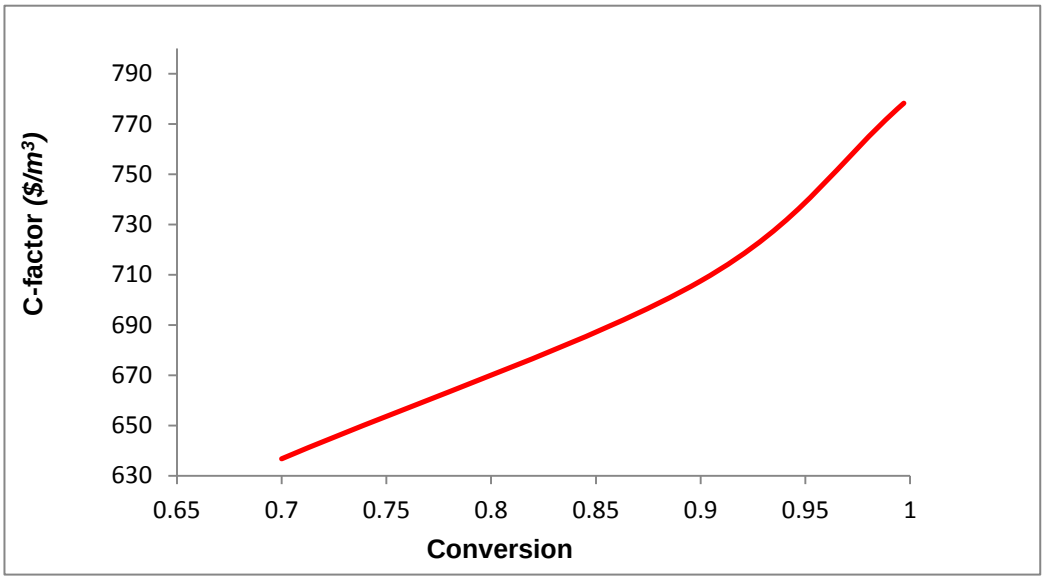

Figure 4

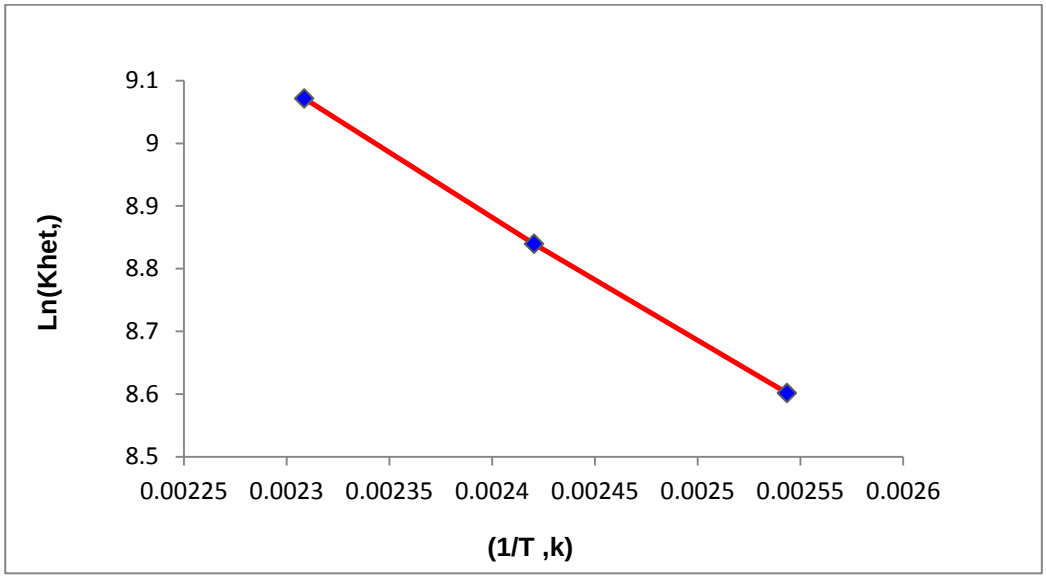
9.1
9
8.9
8.8
8.7
8.6
8.5
Ln(Khet,)
0.00225
0.0023
0.00235
0.0024
0.00245
0.0025
0.00255
0.0026
(1/T ,k)

Figure 5

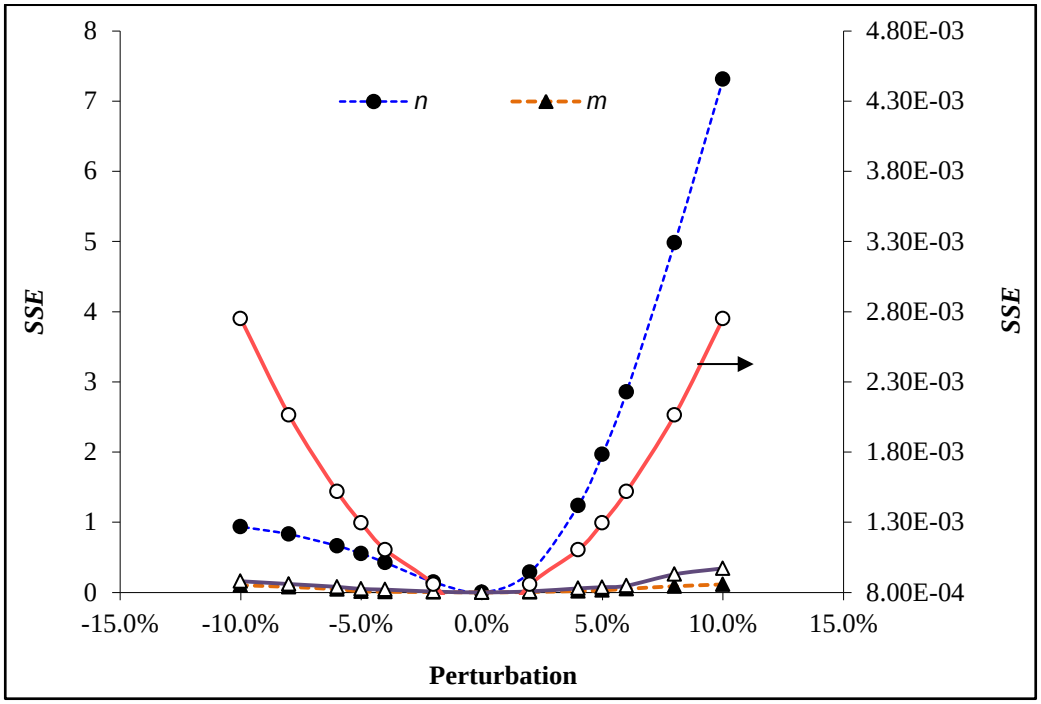
8
7
6
5
4
3
2
1
0
SSE
4.80E-03
4.30E-03
3.80E-03
3.30E-03
2.80E-03
2.30E-03
1.80E-03
1.30E-03
8.00E-04
SSE
n
m
-15.0%
-10.0%
-5.0%
0.0%
5.0%
10.0%
15.0%
Perturbation

Figure 6

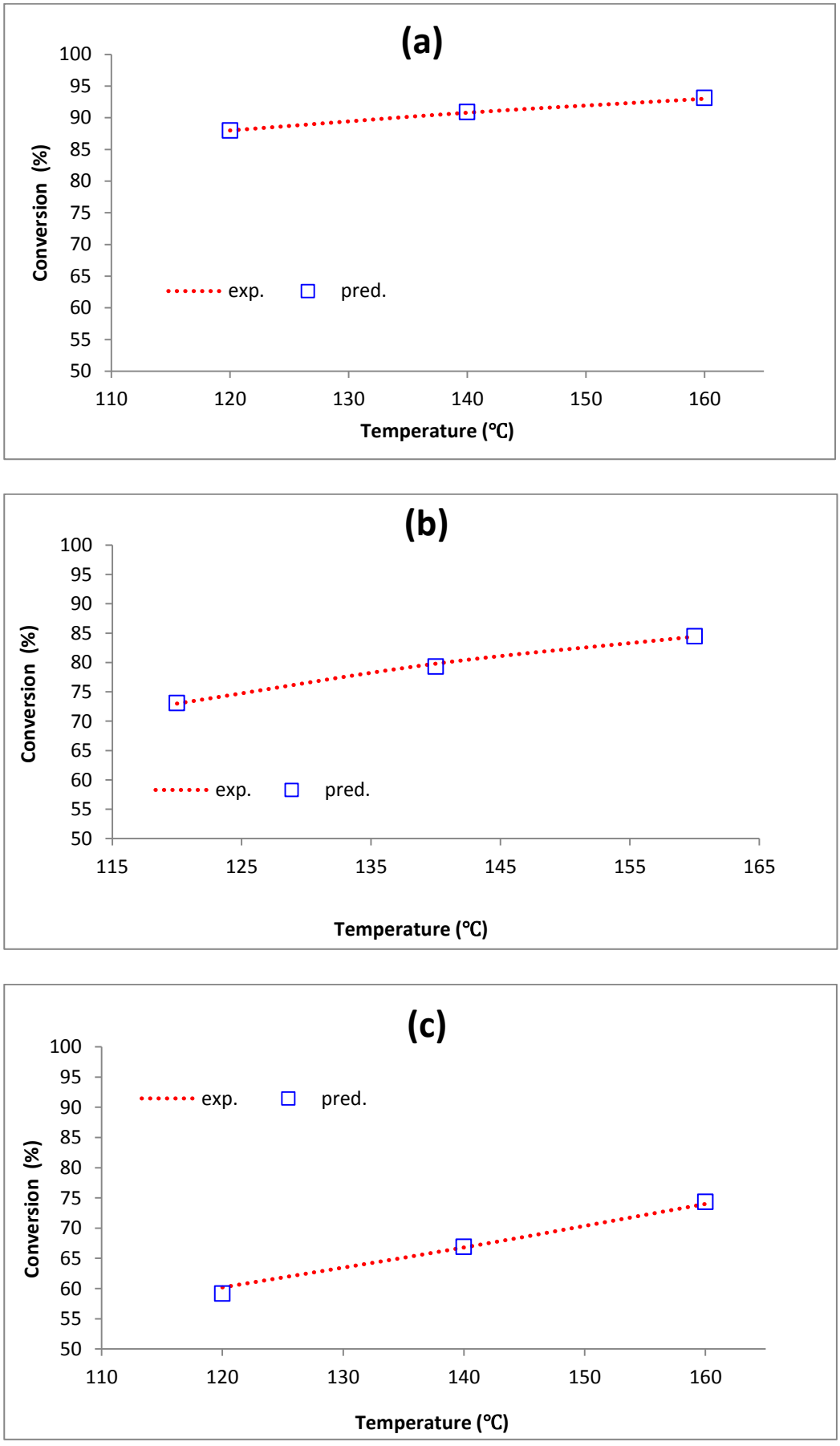
(a)
Conversion (%)
100
95
90
85
80
75
70
65
60
55
50
exp.
pred.
110
120
130
140
150
160
Temperature (℃)
(b)
Conversion (%)
100
95
90
85
80
75
70
65
60
55
50
exp.
pred.
115
125
135
145
155
165
Temperature (℃)
(c)
Conversion (%)
100
95
90
85
80
75
70
65
60
55
50
exp.
pred.
110
120
130
140
150
160
Temperature (℃)

Figure 7

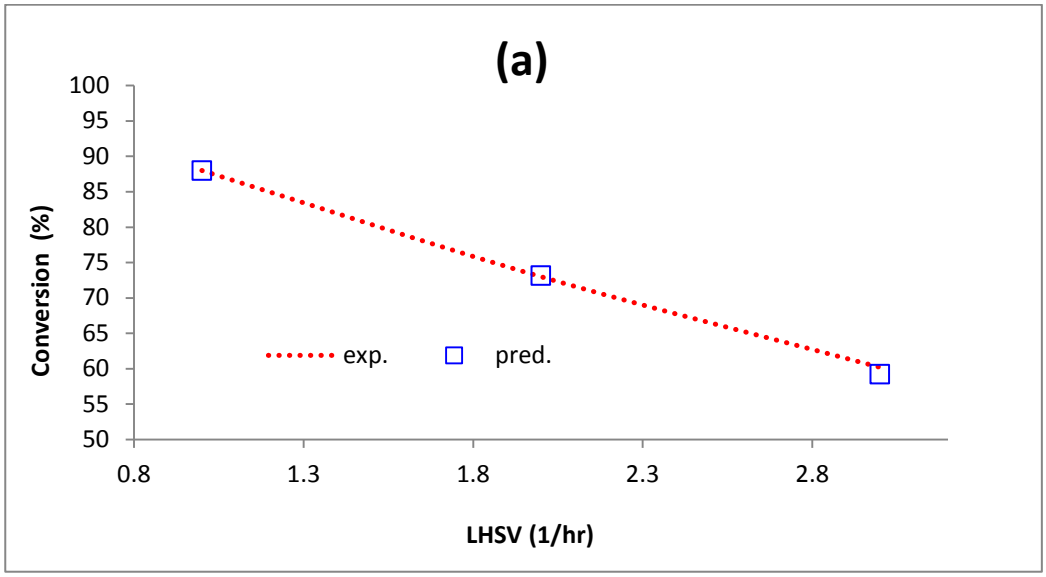
(a)
Conversion (%)
100
95
90
85
80
75
70
65
60
55
50
0.8
1.3
1.8
2.3
2.8
exp.
pred.
LHSV (1/hr)

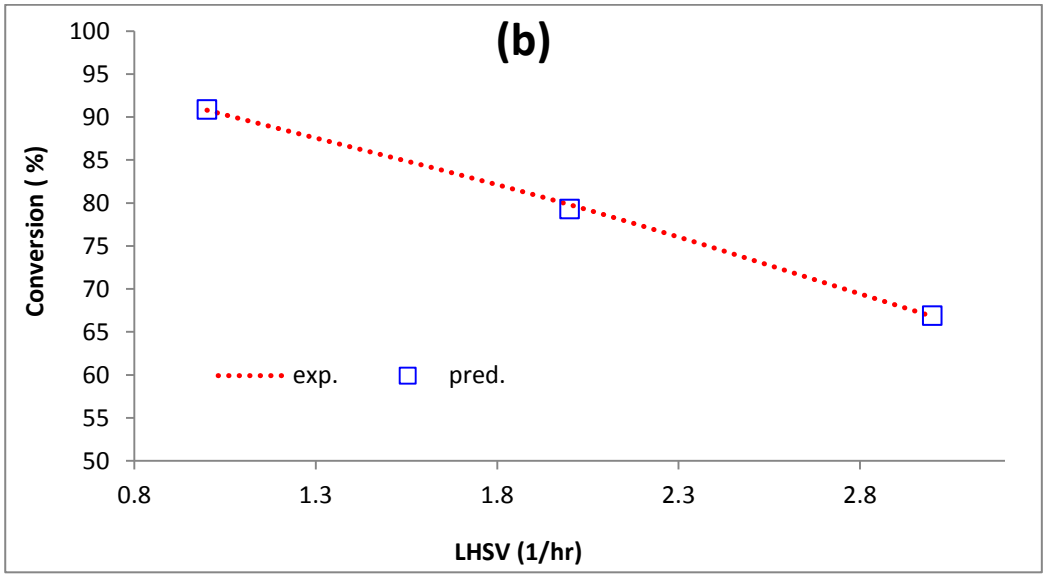
(b)
Conversion (%)
100
95
90
85
80
75
70
65
60
55
50
0.8
1.3
1.8
2.3
2.8
exp.
pred.
LHSV (1/hr)

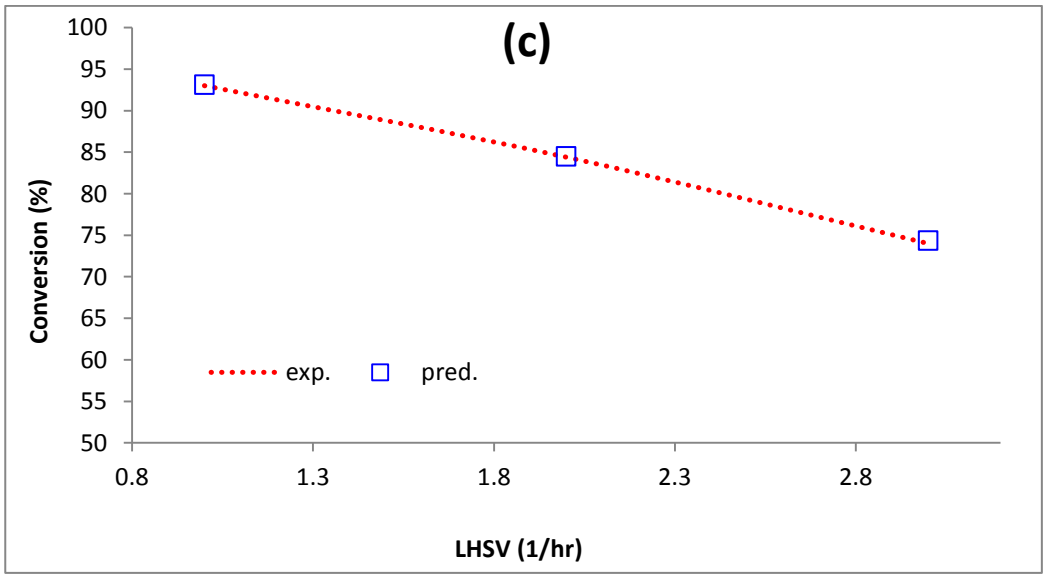
(c)
Conversion (%)
100
95
90
85
80
75
70
65
60
55
50
0.8
1.3
1.8
2.3
2.8
exp.
pred.
LHSV (1/hr)

Figure 8

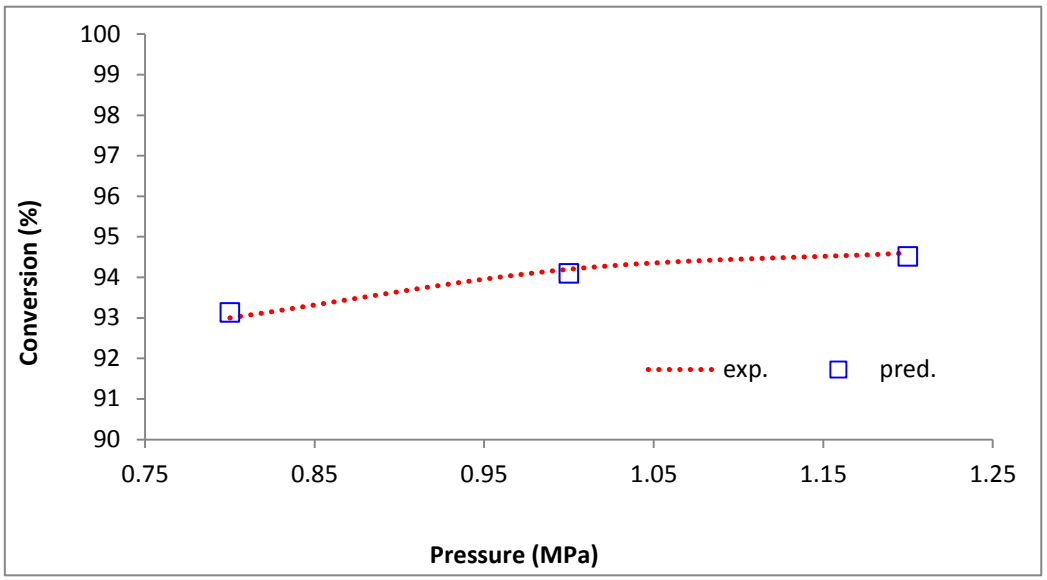

Figure 9

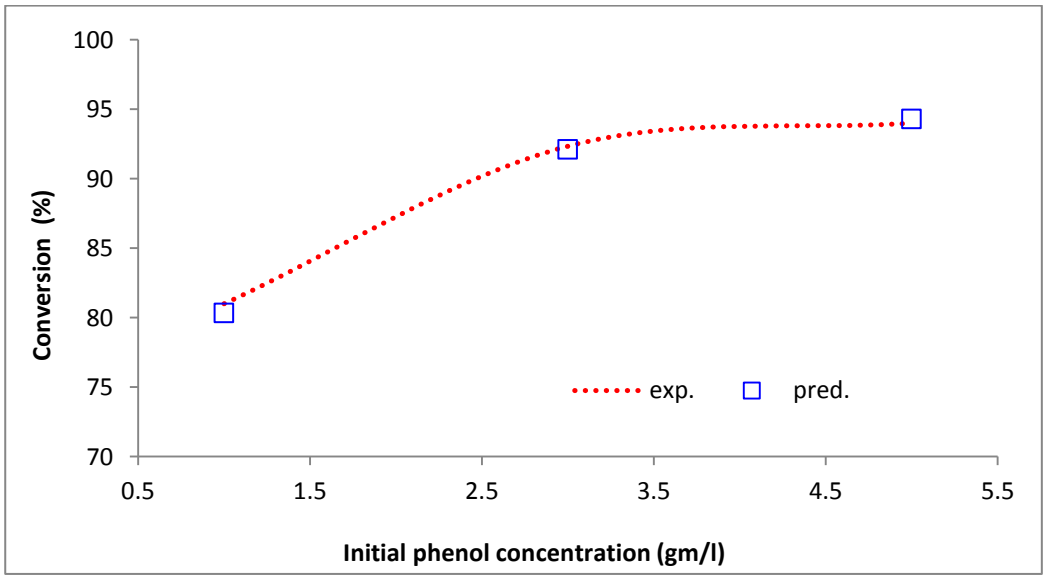

Figure 10

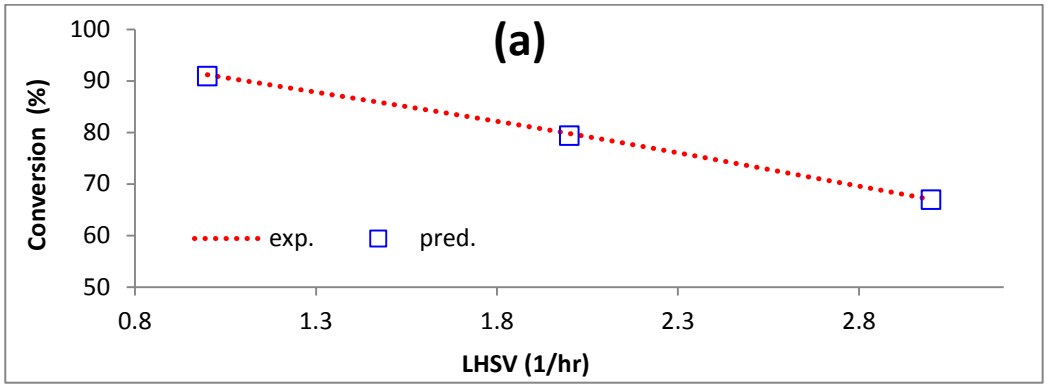
(a)
Conversion (%)
100
90
80
70
60
50
exp.
pred.
0.8
1.3
1.8
2.3
2.8
LHSV (1/hr)

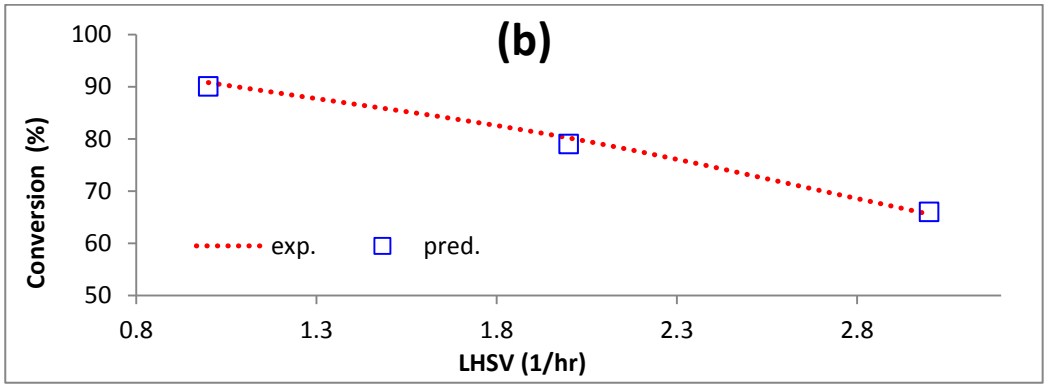
(b)
Conversion (%)
100
90
80
70
60
50
exp.
pred.
0.8
1.3
1.8
2.3
2.8
LHSV (1/hr)

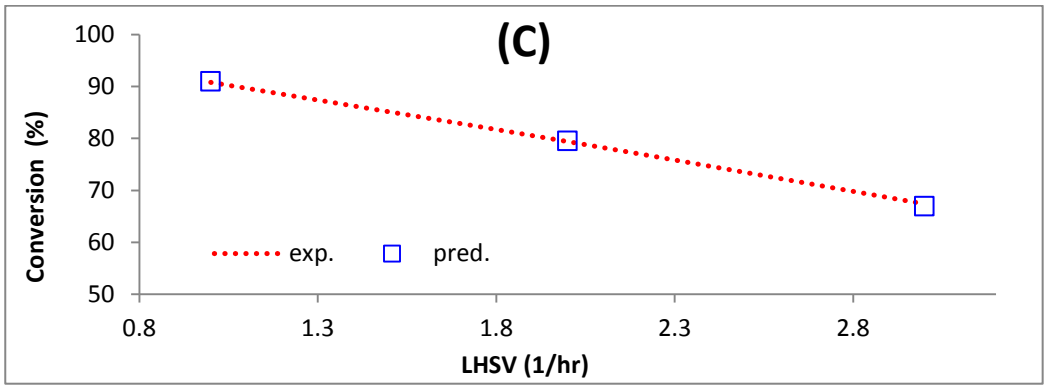
(C)
Conversion (%)
100
90
80
70
60
50
exp.
pred.
0.8
1.3
1.8
2.3
2.8
LHSV (1/hr)

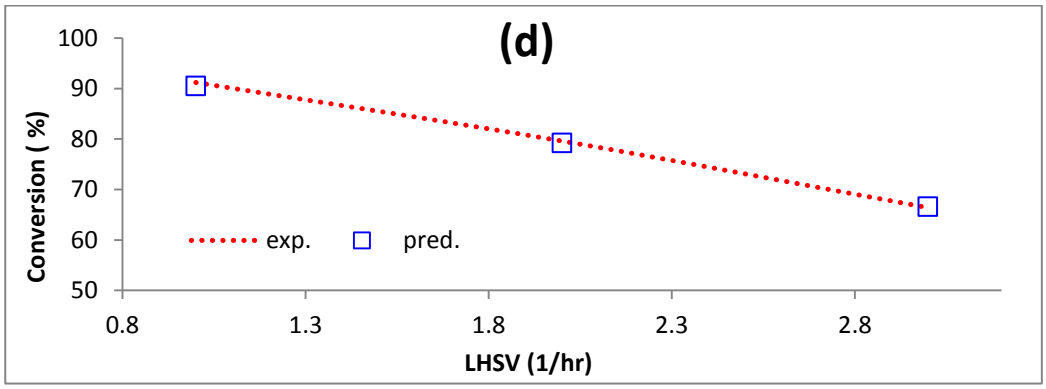
(d)
Conversion (%)
100
90
80
70
60
50
exp.
pred.
0.8
1.3
1.8
2.3
2.8
LHSV (1/hr)

Figure 11